

# Observing Direct CP Violation in Untagged $B$ -Meson Decays

S. Gardner<sup>1\*</sup> and Jusak Tandean<sup>1,2†</sup>

<sup>1</sup>*Department of Physics and Astronomy,  
University of Kentucky,  
Lexington, Kentucky 40506-0055*

*and*

<sup>2</sup>*Department of Physics,  
Southern Methodist University,  
Dallas, Texas 75275-0175<sup>‡</sup>*

## Abstract

Direct CP violation can exist in untagged  $B$ -meson decays to self-conjugate, three-particle final states; it would be realized as a population asymmetry in the untagged decay rate across the mirror line of the Dalitz plot of the three-body decay. We explore the numerical size of this direct CP-violating effect in a variety of  $B$ -meson decays to three pseudoscalar mesons; we show that the resulting asymmetry is comparable to the partial rate asymmetry in the analogous tagged decays, making the search for direct CP violation in the untagged decay rate, for which greater statistics accrue, advantageous.

---

<sup>‡</sup> Present address.

\*Electronic address: [gardner@pa.uky.edu](mailto:gardner@pa.uky.edu)

†Electronic address: [jtandean@mail.physics.smu.edu](mailto:jtandean@mail.physics.smu.edu)

## I. INTRODUCTION

The recent observation of CP violation in the  $B$ -meson system, by dint of the measurement of a nonzero, CP-violating asymmetry in the decay  $B^0(\bar{B}^0) \rightarrow J/\psi K_S$  and related modes [1], opens a new era of discovery. At issue is whether or not CP violation is realized exclusively through a single phase,  $\delta_{KM}$ , in the elements of the Cabibbo-Kobayashi-Maskawa (CKM) matrix [2], as in the standard model (SM). The observed asymmetry, realized through the interference of  $B^0$ - $\bar{B}^0$  mixing and direct decay, is in accord with SM expectations [3], but additional, critical tests of the SM picture have as yet to be realized. For example, the  $B^0(\bar{B}^0) \rightarrow J/\psi K_S$  result, coupled with the hierarchical nature of the CKM matrix [4], suggests that significant direct CP-violating effects ought to exist in the  $B$ -meson system. Moreover, the determined angles of the unitarity triangle, whatever they may be, must be universal, and they must sum to a multiple of  $\pi$  [5]. In this paper, we study a new method of elucidating the presence of direct CP violation. The empirical observation of direct CP violation in the  $B$  system would falsify models in which CP violation is associated overwhelmingly with  $|\Delta B| = 2$ , rather than  $|\Delta B| = 1$ , processes: such models are “essentially” superweak [6–9]. The observation of direct CP violation in the  $B$ -meson system is needed to clarify the nature and origin of CP violation in nature.

Direct CP violation (DCPV) in the  $B$ -meson system is realized if  $|\bar{A}_f/A_f| \neq 1$ , where  $A_f$  is the decay amplitude for  $B \rightarrow f$  and  $\bar{A}_f$  is the decay amplitude for the CP-conjugate process  $\bar{B} \rightarrow \bar{f}$ ; it can be established in a variety of ways. Let us consider the possibilities. Perhaps most familiar is the partial-rate asymmetry,  $\mathcal{A}_{\text{CP}}$ , for which  $\mathcal{A}_{\text{CP}} \propto \Gamma(B \rightarrow f) - \Gamma(\bar{B} \rightarrow \bar{f})$ , with  $\Gamma(B \rightarrow f) \propto |A_f|^2$ . No conclusive evidence for DCPV has been found thus far, although early results in certain modes have been quite suggestive [10–12]. Another pathway to DCPV is realized through the comparison of  $a_{\text{CP}}(f)$ , the CP-violating asymmetry associated with the interference of  $B^0 - \bar{B}^0$  mixing and direct decay, for two different self-conjugate final states  $f$ . Were  $|a_{\text{CP}}(f)| - a_{\text{CP}}(\psi K_S)$  non-zero for a final state  $f$ , one would establish the existence of DCPV, as in the manner of the  $\epsilon'$  parameter in the neutral-kaon system. Indeed, such a difference has been termed  $\epsilon'_B$  [13]. Experimentally, there is no conclusive evidence, as yet, for a nonzero  $\epsilon'_B$  [14, 15]. It is worth noting that  $\epsilon'_B$  can vanish for a specific final state, such as  $\pi^+\pi^-$ , even if DCPV is present in nature [16, 17]. Direct CP violation can also be established through the study of the angular distribution of  $B$  decays into two vector mesons [18], though no empirical limits on the DCPV terms exist as yet. Finally, DCPV can be established through a population asymmetry in the Dalitz plot associated with the untagged decay rate into self-conjugate final states [19], as we will develop in detail. The last two methods have common elements; in particular, neither method requires tagging nor time-dependence to find DCPV in the neutral  $B$ -meson system.

In this paper, we study the method proposed in Ref. [19] to search for DCPV in the decays of neutral, heavy mesons. The method uses untagged, neutral meson decays into self-conjugate final states [20–22] containing more than two hadrons<sup>1</sup>. The multi-particle ( $n > 2$ ) final states realized

---

<sup>1</sup> A note on language: a two-particle, “self-conjugate” state is a CP-eigenstate, whereas a multi-particle ( $n > 2$ ) state is not a CP-eigenstate, in general. Nevertheless, we shall persist in using the phrase “self-conjugate” to describe multi-particle states which “CP self-conjugate states in particle content” [23].

in heavy-meson decays possess a rich resonance structure, entailing the possibility of detecting DCPV without tagging the flavor of the decaying neutral meson. For example, DCPV can occur if we can separate the self-conjugate final state, via the resonances which appear, into distinct, CP-conjugate states. This condition finds its analogue in stereochemistry: we refer to molecules which are non-superimposable, mirror images of each other as enantiomers [24], so that we term non-superimposable, CP-conjugate states as CP-enantiomers [19]. In  $B \rightarrow \pi^+ \pi^- \pi^0$  decay, e.g., the intermediate states  $\rho^+ \pi^-$  and  $\rho^- \pi^+$  form CP-enantiomers, as they are distinct, CP-conjugate states. As a result, the untagged decay rate contains a CP-odd amplitude combination. The empirical presence of this CP-odd interference term in the untagged decay rate would be realized in the Dalitz plot as a population asymmetry, reflective of direct CP violation [19]. The use of untagged decays to search for direct CP violation is also possible in  $B \rightarrow V_1 V_2$  decays; its practical advantage is that there is no loss of statistics due to tagging.

We focus in this paper on the application of this method to untagged  $B$ -meson decays into self-conjugate final states of three pseudoscalar mesons. In Sec. II, we detail, after Ref. [19], how direct CP violation can arise in untagged, neutral- $B$ -meson decays. In Sec. III we discuss how the expected size of the population asymmetry compares, on general grounds, to that of the analogous partial-rate asymmetry. In Sec. IV, we make explicit numerical estimates of the population asymmetries in particular channels and discuss strategies for their experimental realization. In specific, we consider the decays  $B_d \rightarrow \pi^+ \pi^- \pi^0$ ,  $D^+ D^- \pi^0$ , as well as the analogous decays  $B_s \rightarrow K^+ K^- \pi^0$ ,  $D_s^+ D_s^- \pi^0$  in the  $B_s$  system. These final states contain the CP-enantiomers  $\rho^\pm \pi^\mp$ ,  $D^{*\pm} D^\mp$ ,  $K^{*\pm} K^\mp$ , and  $D_s^{*\pm} D_s^\mp$ , respectively. We conclude with a summary and accompanying outlook in Sec. V.

## II. DIRECT CP VIOLATION IN UNTAGGED $B$ DECAYS

### A. $B \rightarrow \rho \pi \rightarrow \pi^+ \pi^- \pi^0$

We follow Ref. [19] and use the decay  $B \rightarrow \rho \pi \rightarrow \pi^+ \pi^- \pi^0$  as a paradigm to illustrate how direct CP violation can occur in untagged, neutral heavy-meson decays. We express the amplitudes for  $B^0 (\bar{B}^0) \rightarrow \rho^+ \pi^-, \rho^- \pi^+, \rho^0 \pi^0$  decay as

$$\mathcal{M}_{\rho^k \pi^l} = a_{kl} \varepsilon_\rho^* \cdot p_\pi \quad \text{and} \quad \bar{\mathcal{M}}_{\rho^k \pi^l} = \bar{a}_{kl} \varepsilon_\rho^* \cdot p_\pi , \quad (1)$$

respectively. Under an assumption of  $\rho$  dominance, the amplitudes for  $B^0 (\bar{B}^0) \rightarrow \pi^+(p_+) \pi^-(p_-) \pi^0(p_0)$  decay can be written as [25, 26]

$$\begin{aligned} \mathcal{M}_{3\pi} &= a_{+-} f_+ + a_{-+} f_- + a_{00} f_0 = a_g f_g + a_u f_u + a_n f_n , \\ \bar{\mathcal{M}}_{3\pi} &= \bar{a}_{+-} f_+ + \bar{a}_{-+} f_- + \bar{a}_{00} f_0 = \bar{a}_g f_g + \bar{a}_u f_u + \bar{a}_n f_n , \end{aligned} \quad (2)$$

where we have summed over the  $\rho$  polarization. We define

$$\begin{aligned} a_g &= a_{+-} + a_{-+} , & a_u &= a_{+-} - a_{-+} , & a_n &= 2 a_{00} , \\ \bar{a}_g &= \bar{a}_{+-} + \bar{a}_{-+} , & \bar{a}_u &= \bar{a}_{+-} - \bar{a}_{-+} , & \bar{a}_n &= 2 \bar{a}_{00} , \end{aligned} \quad (3)$$

and

$$\begin{aligned} f_{\pm} &= \pm \frac{1}{2}(s_{+-} - s_{\mp 0}) \Gamma_{\rho\pi\pi}(s_{\pm 0}) , & f_0 &= \frac{1}{2}(s_{-0} - s_{+0}) \Gamma_{\rho\pi\pi}(s_{+-}) , \\ 2f_g &= f_+ + f_- , & 2f_u &= f_+ - f_- , & 2f_n &= f_0 . \end{aligned} \quad (4)$$

Note that  $\Gamma_{\rho\pi\pi}(s)$  is the  $\rho \rightarrow \pi\pi$  vertex function, which can be determined from  $e^+e^- \rightarrow \pi^+\pi^-$  data, and that  $s_{kl} \equiv (p_k + p_l)^2$ . Let us consider the untagged decay width:

$$\Gamma_{3\pi} = \int \frac{ds_{+0} ds_{-0}}{256\pi^3 m_{B^0}^3} \left( |\mathcal{M}_{3\pi}|^2 + |\bar{\mathcal{M}}_{3\pi}|^2 \right) = \Gamma_{3\pi}^{(1)} + \Gamma_{3\pi}^{(2)} + \Gamma_{3\pi}^{(3)} . \quad (5)$$

We can separate this width into pieces which contain CP-even, as well as CP-odd, amplitude combinations, so that

$$\Gamma_{3\pi}^{(1)} = \int d\Phi \left\{ \sum_{\kappa=g,u,n} \left( |a_{\kappa}|^2 + |\bar{a}_{\kappa}|^2 \right) |f_{\kappa}|^2 + 2 \operatorname{Re} \left[ (a_g^* a_n + \bar{a}_g^* \bar{a}_n) f_g^* f_n \right] \right\} , \quad (6)$$

whereas

$$\Gamma_{3\pi}^{(2)} = \int d\Phi 2 \operatorname{Re} \left[ (a_g^* a_u + \bar{a}_g^* \bar{a}_u) f_g^* f_u \right] , \quad \Gamma_{3\pi}^{(3)} = \int d\Phi 2 \operatorname{Re} \left[ (a_u^* a_n + \bar{a}_u^* \bar{a}_n) f_u^* f_n \right] , \quad (7)$$

with

$$d\Phi \equiv \frac{ds_{+0} ds_{-0}}{256\pi^3 m_{B^0}^3} . \quad (8)$$

It is worth emphasizing that the  $f_k$  are known functions, as  $\Gamma_{\rho\pi\pi}(s)$  itself can be determined from data. Consequently, the coefficients of  $f_k^* f_l$  are observables: they can, in principle, be determined from the Dalitz plot of the  $\pi^+\pi^-\pi^0$  final state [25, 26].

We now consider the transformation properties of the  $a_{ij}$  amplitudes under CP. Under the conventions we detail in Sec. II B, we have

$$a_{+-} \xleftrightarrow{CP} \bar{a}_{-+} , \quad a_{-+} \xleftrightarrow{CP} \bar{a}_{+-} , \quad a_{00} \xleftrightarrow{CP} \bar{a}_{00} , \quad (9)$$

which translate into

$$a_g \xleftrightarrow{CP} +\bar{a}_g , \quad a_u \xleftrightarrow{CP} -\bar{a}_u , \quad a_n \xleftrightarrow{CP} +\bar{a}_n . \quad (10)$$

It follows that the combination  $a_g^* a_n + \bar{a}_g^* \bar{a}_n$  in Eq. (6) is CP even, whereas the combinations

$$a_g^* a_u + \bar{a}_g^* \bar{a}_u \quad \text{and} \quad a_u^* a_n + \bar{a}_u^* \bar{a}_n \quad (11)$$

in Eq. (7) are CP odd, as first noted by Quinn and Silva [26]. The discernable presence of either of the last two combinations signals direct CP violation. These quantities can be measured with the aid of the Dalitz plot of  $s_{+0}$  vs.  $s_{-0}$ , as illustrated in Fig. 1. To see how this is useful, note that under  $p_+ \leftrightarrow p_-$  we have, from Eq. (4), that

$$f_{g,n}(s_{+0}, s_{-0}) = -f_{g,n}(s_{-0}, s_{+0}) , \quad f_u(s_{+0}, s_{-0}) = +f_u(s_{-0}, s_{+0}) , \quad (12)$$

which implies that  $f_g^* f_u$  and  $f_u^* f_n$  are both odd under the interchange  $s_{+0} \leftrightarrow s_{-0}$ , whereas  $f_g^* f_n$  is even. Thus the CP-odd terms make no contribution whatsoever to the total, untagged decay rate; the behavior of Eq. (12) ensures that these contributions vanish identically in the integral over phase space. However, they do generate a population asymmetry about the  $s_{+0} = s_{-0}$  line in the  $3\pi$  Dalitz plot. Explicitly, noting Eqs. (6) and (7), we have

$$\Gamma_{3\pi}^{(1)}[s_{+0} > s_{-0}] = +\Gamma_{3\pi}^{(1)}[s_{+0} < s_{-0}] , \quad \Gamma_{3\pi}^{(2,3)}[s_{+0} > s_{-0}] = -\Gamma_{3\pi}^{(2,3)}[s_{+0} < s_{-0}] , \quad (13)$$

where the inequalities within the square brackets indicate the regions of integration within the Dalitz plot. The corresponding asymmetry can be expressed as

$$\mathcal{A}_{3\pi} \equiv \frac{\Gamma_{3\pi}[s_{+0} > s_{-0}] - \Gamma_{3\pi}[s_{+0} < s_{-0}]}{\Gamma_{3\pi}[s_{+0} > s_{-0}] + \Gamma_{3\pi}[s_{+0} < s_{-0}]} = \frac{\Gamma_{3\pi}^{(2)}[s_{+0} > s_{-0}] + \Gamma_{3\pi}^{(3)}[s_{+0} > s_{-0}]}{\Gamma_{3\pi}^{(1)}[s_{+0} > s_{-0}]} . \quad (14)$$

A nonvanishing value of  $\mathcal{A}_{3\pi}$  reflects direct CP violation in the  $B \rightarrow \rho\pi$  amplitudes. The individual asymmetries,

$$\mathcal{A}_{3\pi}^{(2)} \equiv \frac{\Gamma_{3\pi}^{(2)}[s_{+0} > s_{-0}]}{\Gamma_{3\pi}^{(1)}[s_{+0} > s_{-0}]} , \quad \mathcal{A}_{3\pi}^{(3)} \equiv \frac{\Gamma_{3\pi}^{(3)}[s_{+0} > s_{-0}]}{\Gamma_{3\pi}^{(1)}[s_{+0} > s_{-0}]} , \quad (15)$$

are distinguishable through their location in the Dalitz plot; moreover, they are proportional to different combinations of weak amplitudes, as clear from Eq. (7). The  $f_k$  functions embedded in the definitions of  $\Gamma_{3\pi}^{(2,3)}$  ensure that the population asymmetry is restricted to the  $\rho^k$  bands. In specific,  $\Gamma_{3\pi}^{(2)}$  is non-zero if the population of the  $\rho^+$  band for  $s_{-0} > s_{+0}$  is different from that of the  $\rho^-$  band for  $s_{-0} < s_{+0}$ , whereas  $\Gamma_{3\pi}^{(3)}$  is non-zero if the population of the  $\rho^+ - \rho^0$  interference region, which occurs for  $s_{-0} > s_{+0}$ , is different from that of the  $\rho^- - \rho^0$  interference region, which occurs for  $s_{-0} < s_{+0}$ . It turns out that  $\Gamma_{3\pi}^{(3)}$  is sufficiently small, on general grounds, that its impact on  $\Gamma_{3\pi}^{(2)}$  is negligible.

We have illustrated how DCPV can occur in the untagged decay rate. The untagged decay rate is distinct from the untagged combination of time-dependent rates. To appreciate the consequences of this, we consider the time dependence of neutral,  $B$ -meson decay. We let  $|B^0(t)\rangle$  denote the state which is tagged as a  $B^0$  meson at time  $t = 0$ . We define the mass eigenstates under the weak interaction as  $|B_H\rangle = p|B^0\rangle - q|\bar{B}^0\rangle$  and  $|B_L\rangle = p|B^0\rangle + q|\bar{B}^0\rangle$ ; we denote their masses and widths by  $M_{H,L}$  and  $\Gamma_{H,L}$ , respectively. Denoting  $\mathcal{M}_f(t)$  ( $\bar{\mathcal{M}}_f(t)$ ) as the decay amplitude for  $B^0(t)$  ( $\bar{B}^0(t)$ )  $\rightarrow f$  decay, and assuming mixing CP-violation to be negligible, so that  $|q/p| = 1$ , we have [27, 28]

$$\begin{aligned} |\mathcal{M}_f(t)|^2 &= e^{-\Gamma t} \left[ \frac{1}{2} \left( |\mathcal{M}_f|^2 + |\bar{\mathcal{M}}_f|^2 \right) \cosh \frac{\Delta\Gamma t}{2} + \frac{1}{2} \left( |\mathcal{M}_f|^2 - |\bar{\mathcal{M}}_f|^2 \right) \cos(\Delta M t) \right. \\ &\quad \left. + \text{Re} \left( \frac{q}{p} \mathcal{M}_f^* \bar{\mathcal{M}}_f \right) \sinh \frac{\Delta\Gamma t}{2} - \text{Im} \left( \frac{q}{p} \mathcal{M}_f^* \bar{\mathcal{M}}_f \right) \sin(\Delta M t) \right] , \end{aligned} \quad (16)$$

and

$$\begin{aligned} |\bar{\mathcal{M}}_f(t)|^2 &= e^{-\Gamma t} \left[ \frac{1}{2} \left( |\mathcal{M}_f|^2 + |\bar{\mathcal{M}}_f|^2 \right) \cosh \frac{\Delta\Gamma t}{2} - \frac{1}{2} \left( |\mathcal{M}_f|^2 - |\bar{\mathcal{M}}_f|^2 \right) \cos(\Delta M t) \right. \\ &\quad \left. + \text{Re} \left( \frac{q}{p} \mathcal{M}_f^* \bar{\mathcal{M}}_f \right) \sinh \frac{\Delta\Gamma t}{2} + \text{Im} \left( \frac{q}{p} \mathcal{M}_f^* \bar{\mathcal{M}}_f \right) \sin(\Delta M t) \right] . \end{aligned} \quad (17)$$

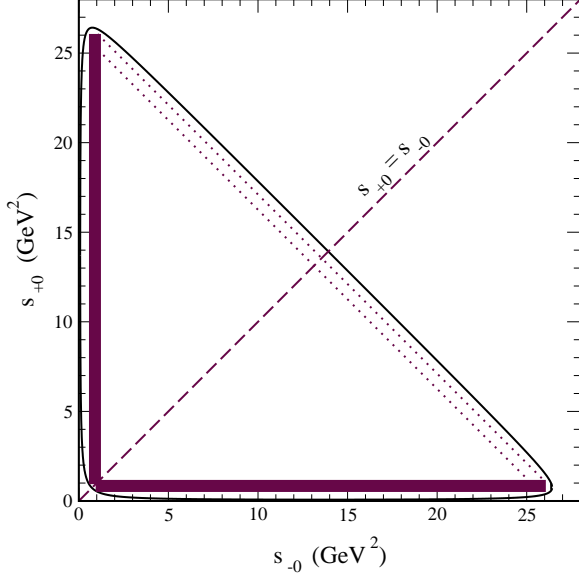


FIG. 1: The allowed Dalitz region for  $B^0, \bar{B}^0 \rightarrow \pi^+ \pi^- \pi^0$  decay. The decays mediated by the  $\rho^\pm \pi^\mp$  intermediate states dominate the Dalitz plot; their location is indicated schematically by the shaded bands. The  $\rho^0$  band, reflective of the  $\rho^0 \pi^0$  intermediate state, is indicated schematically by the dotted lines. An asymmetry in the population of the Dalitz plot about the  $s_{+0} = s_{-0}$  “mirror line” signals direct CP violation. Note that the asymmetries  $\mathcal{A}_{3\pi}^{(2)}$  and  $\mathcal{A}_{3\pi}^{(3)}$ , as given in Eq. (15), describe the population asymmetry of the  $\rho^\pm$  bands and that of the overlapping  $\rho^\pm$ - $\rho^0$  bands about the mirror line, respectively.

We have used the conventions of Ref. [28], so that  $2\Gamma \equiv \Gamma_H + \Gamma_L$  and  $\Delta M \equiv M_H - M_L$ , though we define  $\Delta\Gamma \equiv \Gamma_H - \Gamma_L$ . The untagged combination of time-dependent rates is given by

$$|\mathcal{M}_f(t)|^2 + |\bar{\mathcal{M}}_f(t)|^2 = e^{-\Gamma t} \left[ \left( |\mathcal{M}_f|^2 + |\bar{\mathcal{M}}_f|^2 \right) \cosh \frac{\Delta\Gamma t}{2} + 2 \operatorname{Re} \left( \frac{q}{p} \mathcal{M}_f^* \bar{\mathcal{M}}_f \right) \sinh \frac{\Delta\Gamma t}{2} \right]. \quad (18)$$

The population asymmetry associated with the untagged combination of time-dependent rates need not be a signal of direct CP violation at *non-zero*  $t$ . The population asymmetries are generated by terms of form  $f_g^* f_u$  or  $f_u^* f_n$ , as in Eqs. (7,15); at  $t \neq 0$ ,  $\mathcal{M}_f^* \bar{\mathcal{M}}_f$  enters as well. Such terms are associated with CP-odd amplitudes in  $\operatorname{Re}(\mathcal{M}_f^* \bar{\mathcal{M}}_f)$ , but with CP-even amplitudes in  $\operatorname{Im}(\mathcal{M}_f^* \bar{\mathcal{M}}_f)$ . The pieces of interest in  $\mathcal{M}_f^* \bar{\mathcal{M}}_f$  are of form

$$\mathcal{M}_f^* \bar{\mathcal{M}}_f \Big|_{f_g^* f_u} = a_{gu}^+ \operatorname{Re}(f_g^* f_u) + i a_{gu}^- \operatorname{Im}(f_g^* f_u) \quad (19)$$

where  $a_{gu}^\pm = a_g^* \bar{a}_u \pm a_u^* \bar{a}_g$  and the replacement  $g, u \leftrightarrow u, n$  yields the  $f_u^* f_n$  terms. We note

$$a_{gu}^\pm \xleftrightarrow{CP} \mp a_{gu}^{\pm*}, \quad (20)$$

so that the CP properties of  $(\operatorname{Re}, \operatorname{Im})(\mathcal{M}_f^* \bar{\mathcal{M}}_f)$  follow. Since  $q/p$  is complex,  $\operatorname{Im}(\mathcal{M}_f^* \bar{\mathcal{M}}_f)$  enters  $\operatorname{Re}(q \mathcal{M}_f^* \bar{\mathcal{M}}_f / p)$  as well, so that the population asymmetry associated with this  $t$ -dependent term can be generated by direct CP violation, but does not occur exclusively because of it. In a similar vein, we conclude that a population asymmetry in  $|\mathcal{M}_f(t)|^2 - |\bar{\mathcal{M}}_f(t)|^2$  need not be reflective of

direct CP violation; at  $t = 0$  it is decidedly not. Since  $\Delta\Gamma \ll \Gamma$  in the SM [29], though it is likely more significant in the  $B_s$  system [30, 31]<sup>2</sup>, the practical impact of this observation ought be minor; it nevertheless remains that the population asymmetry signals direct CP violation in the untagged decay rate, rather than in the untagged combination of tagged, time-dependent rates. However, if the latter quantity is integrated in  $t$  over a symmetric region about  $t = 0$ , the undesired term vanishes, and the resulting time-integrated, population asymmetry is also reflective of direct CP violation.

## B. $B \rightarrow \pi^+\pi^-\pi^0$

Herewith we demonstrate that the population asymmetry in the untagged combination of time-independent rates in  $B \rightarrow \pi^+\pi^-\pi^0$  decay is a signature of direct CP violation; we need not confine ourselves to the regions of the Dalitz plot dominated by the  $\rho$  resonance. Indeed, our demonstration follows for all three-body decays which are self-conjugate in particle content; the final-state particles need not be related by isospin symmetry.

Let us consider the amplitude for  $B \rightarrow \pi^+\pi^-\pi^0$  decay. We enumerate the possible contributions by the orbital angular momentum of the final-state mesons, as this suffices to characterize the CP of the final, three-particle state. We note, in passing, that a complete parametrization of the decay of a pseudoscalar meson to  $\pi^+\pi^-\pi^0$  in terms of the isospin  $I$  of the pions and  $|\Delta I|$  of the weak transition can be found in Ref. [32]. The final state must have zero total angular momentum, so that we write  $(\pi_1\pi_2)_l(\pi_3)_l$ , where  $l$  denotes the total orbital angular momentum quantum number of the particles in parentheses, combined to yield a state of total angular momentum zero.<sup>3</sup> We have implicitly summed over the magnetic quantum numbers,  $m$ , possible for fixed  $l$ . The decay mechanism can distinguish the way in which the three pions are coupled to yield a state of total angular momentum zero. For example, in decays mediated by a two-body intermediate state, such as  $B \rightarrow \rho^+\pi^- \rightarrow (\pi^+\pi^0)_1(\pi^-)_1$  or  $B \rightarrow \rho^-\pi^+ \rightarrow (\pi^-\pi^0)_1(\pi^+)_1$ , the differing ways in which two of the three pions are coupled to a  $l = 1$  state reflect distinct weak amplitudes. We denote the amplitude for  $B \rightarrow (\pi^+\pi^0)_1(\pi^-)_1$  decay as  $\mathcal{M}_{+-}(p_+, p_-, p_0)$ , so that the first subscript denotes the net charge of two pions coupled to a  $l = 1$  state and the second subscript denotes the charge of the third pion; its arguments  $p_+, p_-, p_0$  denote the momenta of the  $\pi^+, \pi^-$ , and  $\pi^0$  mesons, respectively, so that we define

$$\begin{aligned} \mathcal{M}_{\pm\mp}^l(p_+, p_-, p_0) &= \left\langle [\pi^\pm(p_\pm)\pi^0(p_0)]_l \pi^\mp(p_\mp)_l \middle| \mathcal{H}_{\text{eff}} \middle| B^0 \right\rangle = \sum_i \lambda_i^* \left\langle (\pi^\pm\pi^0)_l \pi_l^\mp \middle| Q_i^\dagger \middle| B^0 \right\rangle, \\ \mathcal{M}_{00}^l(p_+, p_-, p_0) &= \left\langle [\pi^+(p_+)\pi^-(p_-)]_l \pi^0(p_0)_l \middle| \mathcal{H}_{\text{eff}} \middle| B^0 \right\rangle = \sum_i \lambda_i^* \left\langle (\pi^+\pi^-)_l \pi_l^0 \middle| Q_i^\dagger \middle| B^0 \right\rangle, \end{aligned} \quad (21)$$

---

<sup>2</sup> We note  $\Delta\Gamma_d^{\text{SM}}/\Gamma_d \approx 3 \times 10^{-3}$ , whereas  $\Delta\Gamma_s^{\text{SM}}/\Gamma_s = 0.12 \pm 0.06$ , as per Ref. [28] and references therein.

<sup>3</sup> Note that  $(\pi_3)_l$  denotes the orbital angular angular of  $\pi_3$  with respect to the center-of-mass of the  $\pi_1\pi_2$  system.

with analogous quantities for  $\bar{B}_0$  decay

$$\begin{aligned}\bar{\mathcal{M}}_{\mp\pm}^l(p_+, p_-, p_0) &= \left\langle [\pi^\mp(p_\mp)\pi^0(p_0)]_l \pi^\pm(p_\pm)_l \middle| \mathcal{H}_{\text{eff}} \middle| \bar{B}^0 \right\rangle = \sum_i \lambda_i \left\langle (\pi^\mp\pi^0)_l \pi_l^\pm \middle| Q_i \middle| \bar{B}^0 \right\rangle. \\ \bar{\mathcal{M}}_{00}^l(p_+, p_-, p_0) &= \left\langle [\pi^+(p_+)\pi^-(p_-)]_l \pi^0(p_0)_l \middle| \mathcal{H}_{\text{eff}} \middle| \bar{B}^0 \right\rangle = \sum_i \lambda_i \left\langle (\pi^+\pi^-)_l \pi_l^0 \middle| Q_i \middle| \bar{B}^0 \right\rangle,\end{aligned}\tag{22}$$

where we write the  $|\Delta B| = 1$  effective, weak Hamiltonian as

$$\mathcal{H}_{\text{eff}} = \sum_i \left( \lambda_i Q_i + \lambda_i^* Q_i^\dagger \right).\tag{23}$$

To determine the transformation properties of these amplitudes under CP, we have

$$\begin{aligned}CP|B\rangle &= \eta_B |\bar{B}\rangle, & CP|\pi^0\rangle &= -|\pi^0\rangle, & CP|\pi^+\rangle &= \eta_\pi |\pi^-\rangle, \\ CP Q_i (CP)^\dagger &= \eta_Q Q_i^\dagger,\end{aligned}\tag{24}$$

where  $\eta_{B,\pi,Q}$  are arbitrary phase-factors. Armed with these conventions, we turn to the determination of the CP-properties of the three-meson final state. Working in the rest frame of the two pions coupled to angular momentum  $l$ , we note that

$$P \left| [\pi_1(\mathbf{p}) \pi_2(-\mathbf{p})]_l \pi_3(\mathbf{p}')_l \right\rangle = - \left| [\pi_1(\mathbf{p}) \pi_2(-\mathbf{p})]_l \pi_3(\mathbf{p}')_l \right\rangle,\tag{25}$$

where the minus sign emerges from the negative intrinsic parity of the pseudoscalar mesons. Under charge conjugation,

$$C \left| [\pi^+(\mathbf{p}) \pi^-(\mathbf{p})]_l \pi^0(\mathbf{p}')_l \right\rangle = \left| [\pi^-(\mathbf{p}) \pi^+(\mathbf{p})]_l \pi^0(\mathbf{p}')_l \right\rangle = (-1)^l \left| [\pi^-(\mathbf{p}) \pi^+(\mathbf{p})]_l \pi^0(\mathbf{p}')_l \right\rangle.\tag{26}$$

It follows that

$$\begin{aligned}CP \left| [\pi^+(\mathbf{p}) \pi^-(\mathbf{p})]_l \pi^0(\mathbf{p}')_l \right\rangle &= -C \left| [\pi^+(\mathbf{p}) \pi^-(\mathbf{p})]_l \pi^0(\mathbf{p}')_l \right\rangle = (-1)^{l+1} \left| [\pi^-(\mathbf{p}) \pi^+(\mathbf{p})]_l \pi^0(\mathbf{p}')_l \right\rangle \\ CP \left| [\pi^-(\mathbf{p}) \pi^0(\mathbf{p})]_l \pi^+(\mathbf{p}')_l \right\rangle &= - \left| [\pi^+(\mathbf{p}) \pi^0(\mathbf{p})]_l \pi^-(\mathbf{p}')_l \right\rangle.\end{aligned}\tag{27}$$

We thus determine

$$\begin{aligned}\left\langle [\pi^-(p_-) \pi^0(p_0)]_l \pi^+(p_+) \middle| Q_i \middle| \bar{B}^0 \right\rangle &= \left\langle [\pi^-(p_-) \pi^0(p_0)]_l \pi^+(p_+) \middle| (CP)^\dagger CP Q_i (CP)^\dagger CP \middle| \bar{B}^0 \right\rangle \\ &= -\eta_B^* \eta_Q \left\langle [\pi^+(p_-) \pi^0(p_0)]_l \pi^-(p_+) \middle| Q_i^\dagger \middle| B^0 \right\rangle,\end{aligned}\tag{28}$$

where we work in the frame in which  $\mathbf{p}_- = \mathbf{p}$ ,  $\mathbf{p}_0 = -\mathbf{p}$ , and  $\mathbf{p}_+ = \mathbf{p}'$ . Moreover,

$$\begin{aligned}\left\langle (\pi^+\pi^-)_l \pi_l^0 \middle| Q_i \middle| \bar{B}^0 \right\rangle &= \left\langle (\pi^+\pi^-)_l \pi_l^0 \middle| (\mathcal{CP})^\dagger \mathcal{CP} Q_i (\mathcal{CP})^\dagger \mathcal{CP} \middle| \bar{B}^0 \right\rangle \\ &= \eta_B^* \eta_Q (-1)^{l+1} \left\langle (\pi^+\pi^-)_l \pi_l^0 \middle| Q_i^\dagger \middle| B^0 \right\rangle,\end{aligned}\tag{29}$$

where  $\mathbf{p}_- = \mathbf{p}$ ,  $\mathbf{p}_+ = -\mathbf{p}$ , and  $\mathbf{p}_0 = \mathbf{p}'$ . The determined CP properties are independent of frame, so that we conclude, more generally, that<sup>4</sup>

$$\begin{aligned}\bar{\mathcal{M}}_{-+}^l(p_+, p_-, p_0) &= -\eta_B^* \eta_Q \sum_i \lambda_i \left\langle [\pi^+(p_-) \pi^0(p_0)]_l \pi^-(p_+) \right| Q_i^\dagger \left| B^0 \right\rangle, \\ \bar{\mathcal{M}}_{+-}^l(p_+, p_-, p_0) &= -\eta_B^* \eta_Q \sum_i \lambda_i \left\langle [\pi^-(p_+) \pi^0(p_0)]_l \pi^+(p_-) \right| Q_i^\dagger \left| B^0 \right\rangle, \\ \bar{\mathcal{M}}_{00}^l(p_+, p_-, p_0) &= \eta_B^* \eta_Q (-1)^{l+1} \sum_i \lambda_i \left\langle (\pi^+(p_+) \pi^-(p_-))_l \pi^0(p_0)_l \right| Q_i^\dagger \left| B^0 \right\rangle,\end{aligned}\quad (30)$$

or that

$$\begin{aligned}\bar{\mathcal{M}}_{-+}^l(p_+, p_-, p_0) &\xrightarrow{CP} -\eta_B^* \eta_Q \mathcal{M}_{+-}^l(p_-, p_+, p_0) \\ \bar{\mathcal{M}}_{+-}^l(p_+, p_-, p_0) &\xrightarrow{CP} -\eta_B^* \eta_Q \mathcal{M}_{-+}^l(p_-, p_+, p_0) \\ \bar{\mathcal{M}}_{00}^l(p_+, p_-, p_0) &\xrightarrow{CP} -\eta_B^* \eta_Q \mathcal{M}_{00}^l(p_-, p_+, p_0),\end{aligned}\quad (31)$$

where the  $(-1)^l$  in the last line of Eq. (30) has been absorbed through the exchange  $p_+ \leftrightarrow p_-$ . Thus we observe that the CP transformation is tied to the mirror transformation of the Dalitz plot,  $p_+ \leftrightarrow p_-$ .<sup>5</sup> Generalizing the definitions of Eq. (3), we introduce

$$\begin{aligned}\mathcal{M}_g^l(p_+, p_-, p_0) &= \frac{1}{2} \left[ \mathcal{M}_{+-}^l(p_+, p_-, p_0) + \mathcal{M}_{-+}^l(p_+, p_-, p_0) \right. \\ &\quad \left. + (-1)^l \mathcal{M}_{+-}^l(p_-, p_+, p_0) + (-1)^l \mathcal{M}_{-+}^l(p_-, p_+, p_0) \right], \\ \mathcal{M}_u^l(p_+, p_-, p_0) &= \frac{1}{2} \left[ \mathcal{M}_{+-}^l(p_+, p_-, p_0) + \mathcal{M}_{-+}^l(p_+, p_-, p_0) \right. \\ &\quad \left. - (-1)^l \mathcal{M}_{+-}^l(p_-, p_+, p_0) - (-1)^l \mathcal{M}_{-+}^l(p_-, p_+, p_0) \right], \\ \mathcal{M}_n^l(p_+, p_-, p_0) &= \mathcal{M}_{00}^l(p_+, p_-, p_0),\end{aligned}\quad (32)$$

and

---

<sup>4</sup> We can check the CP assignments by determining the CP of associated, two-body modes. Noting  $CP|\rho^0\rangle = +|\rho^0\rangle$  and  $CP|\rho^+\rangle = \eta_\rho|\rho^-\rangle$ , we find  $\langle \pi^0(p_0)\rho^0(p_\rho) | Q_i | \bar{B}^0 \rangle = \eta_B^* \eta_Q \langle \pi^0(p_0)\rho^0(p_\rho) | Q_i^\dagger | B^0 \rangle$ , as well as  $\langle \pi^+(p_+) \pi^-(p_-) | \mathcal{H}_{\text{str}} | \rho^0(p_\rho) \rangle = \langle \pi^+(p_+) \pi^-(p_-) | \mathcal{H}_{\text{str}}^\dagger | \rho^0(p_\rho) \rangle$ , where  $p_\rho = p_+ + p_-$  and  $\mathbf{p}_\rho = \mathbf{0}$ . Moreover,  $\langle \pi^+(p_+) (\rho^-(p_\rho)) | Q_i | \bar{B}^0 \rangle = -\eta_B^* \eta_Q \eta_\rho^* \eta_\pi \langle \pi^-(p_+) \rho^+(p_\rho) | Q_i^\dagger | B^0 \rangle$  and  $\langle \pi^-(p_-) \pi^0(p_0) | \mathcal{H}_{\text{str}} | \rho^-(p_\rho) \rangle = \eta_\rho \eta_\pi^* \langle \pi^+(p_-) \pi^0(p_0) | \mathcal{H}_{\text{str}}^\dagger | \rho^+(p_\rho) \rangle$ , where  $p_\rho = p_- + p_0$  and  $\mathbf{p}_\rho = \mathbf{0}$ . Of course  $\mathcal{H}_{\text{str}} = \mathcal{H}_{\text{str}}^\dagger$ . Removing the matrix elements associated with  $\rho \rightarrow \rho\pi$ , we see that  $B \rightarrow \rho\pi$  transformation properties extracted from Eq. (30) are in accord with our direct calculation. Choosing, in addition,  $\eta_B^* \eta_Q = +1$  and  $\eta_\rho^* \eta_\pi = -1$  yields Eq. (9).

<sup>5</sup> We can use the amplitudes of Sec. II A to check Eq. (31). Choosing  $\eta_B^* \eta_Q = +1$  and noting  $f_\pm \xrightarrow{p_\pm \leftrightarrow p_-} -f_\mp$  and  $f_0 \xrightarrow{p_\pm \leftrightarrow p_-} -f_0$ , so that  $\mathcal{M}_{3\pi}(p_+, p_-, p_0) = a_{+-} f_+ + a_{-+} f_- + a_{00} f_0$  does yield  $\bar{\mathcal{M}}_{3\pi}(p_+, p_-, p_0) = \bar{a}_{+-} f_+ + \bar{a}_{-+} f_- + \bar{a}_{00} f_0$  upon CP transformation, as per Eq. (2).

$$\begin{aligned}
\bar{\mathcal{M}}_g^l(p_+, p_-, p_0) &= \frac{1}{2} \left[ \bar{\mathcal{M}}_{+-}^l(p_+, p_-, p_0) + \bar{\mathcal{M}}_{-+}^l(p_+, p_-, p_0) \right. \\
&\quad \left. + (-1)^l \bar{\mathcal{M}}_{+-}^l(p_-, p_+, p_0) + (-1)^l \bar{\mathcal{M}}_{-+}^l(p_-, p_+, p_0) \right] , \\
\bar{\mathcal{M}}_u^l(p_+, p_-, p_0) &= \frac{1}{2} \left[ \bar{\mathcal{M}}_{+-}^l(p_+, p_-, p_0) + \bar{\mathcal{M}}_{-+}^l(p_+, p_-, p_0) \right. \\
&\quad \left. - (-1)^l \bar{\mathcal{M}}_{+-}^l(p_-, p_+, p_0) - (-1)^l \bar{\mathcal{M}}_{-+}^l(p_-, p_+, p_0) \right] , \\
\bar{\mathcal{M}}_n^l(p_+, p_-, p_0) &= \bar{\mathcal{M}}_{00}^l(p_+, p_-, p_0) ,
\end{aligned} \tag{33}$$

where we note<sup>6</sup>

$$\begin{aligned}
\bar{\mathcal{M}}_g^l(p_+, p_-, p_0) &\xleftrightarrow{CP} -\eta_B^* \eta_Q \mathcal{M}_g^l(p_-, p_+, p_0) , \quad \bar{\mathcal{M}}_u^l(p_+, p_-, p_0) \xleftrightarrow{CP} -\eta_B^* \eta_Q \mathcal{M}_u^l(p_-, p_+, p_0) , \\
\bar{\mathcal{M}}_n^l(p_+, p_-, p_0) &\xleftrightarrow{CP} -\eta_B^* \eta_Q \mathcal{M}_n^l(p_-, p_+, p_0) .
\end{aligned} \tag{34}$$

To exploit these transformation properties, we parametrize the  $B \rightarrow \pi^+ \pi^- \pi^0$  amplitude as

$$\mathcal{M}_{3\pi}(p_+, p_-, p_0) = \sum_{l=0}^{\infty} (\mathcal{M}_{+-}^l + \mathcal{M}_{-+}^l + \mathcal{M}_{00}^l) = \sum_{l=0}^{\infty} (\mathcal{M}_g^l + \mathcal{M}_u^l + \mathcal{M}_n^l) , \tag{35}$$

where we have suppressed the common arguments throughout, so that  $\mathcal{M}_{\pm\mp}^l$  is, indeed,  $\mathcal{M}_{\pm\mp}^l(p_+, p_-, p_0)$ . Analogously, for the  $\bar{B} \rightarrow \pi^+ \pi^- \pi^0$  amplitude we have

$$\bar{\mathcal{M}}_{3\pi}(p_+, p_-, p_0) = \sum_{l=0}^{\infty} (\bar{\mathcal{M}}_{+-}^l + \bar{\mathcal{M}}_{-+}^l + \bar{\mathcal{M}}_{00}^l) = \sum_{l=0}^{\infty} (\bar{\mathcal{M}}_g^l + \bar{\mathcal{M}}_u^l + \bar{\mathcal{M}}_n^l) . \tag{36}$$

A two-body decay mechanism distinguishes the terms of fixed  $l$ ; however, our parametrization is not limited by this assumption. Note that  $\mathcal{M}_{+-}^l(p_+, p_-, p_0)$ , e.g., includes the product  $a_{+-} f_+$  of Sec. II A. With these definitions the untagged decay rate can be written

$$|\mathcal{M}_{3\pi}|^2 + |\bar{\mathcal{M}}_{3\pi}|^2 = \sum_{\kappa \in g, u, n} \sum_{j, l=0}^{\infty} \left[ (\mathcal{M}_{\kappa}^{j*} \mathcal{M}_{\kappa}^l + \bar{\mathcal{M}}_{\kappa}^{j*} \bar{\mathcal{M}}_{\kappa}^l) + 2 \sum_{\lambda > \kappa} \text{Re}(\mathcal{M}_{\kappa}^{j*} \mathcal{M}_{\lambda}^l + \bar{\mathcal{M}}_{\kappa}^{j*} \bar{\mathcal{M}}_{\lambda}^l) \right] , \tag{37}$$

where  $\lambda \in g, u, n$  and  $\lambda > \kappa$  means that the  $g, u, n$  subscripts are not repeated. Applying Eq. (34), we observe that

$$|\mathcal{M}_{3\pi}|^2(p_+, p_-, p_0) + |\bar{\mathcal{M}}_{3\pi}|^2(p_+, p_-, p_0) \xleftrightarrow{CP} |\mathcal{M}_{3\pi}|^2(p_-, p_+, p_0) + |\bar{\mathcal{M}}_{3\pi}|^2(p_-, p_+, p_0) , \tag{38}$$

so that the untagged decay width,  $\Gamma_{3\pi}$ , realized from integrating Eq. (37) over the invariant phase space, as in Eq. (5), is a manifestly CP-even quantity. This follows because the integration region

---

<sup>6</sup> We can use the amplitudes of Sec. II A to check Eq. (34) as well. Choosing  $\eta_B^* \eta_Q = +1$ , we see  $f_g \xleftrightarrow{p_+ \leftrightarrow p_-} -f_g$  and  $f_u \xleftrightarrow{p_+ \leftrightarrow p_-} +f_u$ , so that  $\mathcal{M}_{3\pi}(p_+, p_-, p_0) = a_g f_g + a_u f_u + a_n f_n$  does yield  $\bar{\mathcal{M}}_{3\pi}(p_+, p_-, p_0) = \bar{a}_g f_g + \bar{a}_u f_u + \bar{a}_n f_n$  under CP transformation, as per Eq. (2).

is itself  $p_+ \leftrightarrow p_-$  symmetric. The population asymmetry, however, allows us to observe direct CP violation. Forming

$$\mathcal{A}_{3\pi} \equiv \frac{\Gamma_{3\pi}[s_{+0} > s_{-0}] - \Gamma_{3\pi}[s_{+0} < s_{-0}]}{\Gamma_{3\pi}[s_{+0} > s_{-0}] + \Gamma_{3\pi}[s_{+0} < s_{-0}]}, \quad (39)$$

where

$$\begin{aligned} \Gamma_{3\pi}[s_{+0} > s_{-0}] - \Gamma_{3\pi}[s_{+0} < s_{-0}] &= \int_{s_{+0} > s_{-0}} d\Phi \{ [|\mathcal{M}_{3\pi}|^2(p_+, p_-, p_0) + |\bar{\mathcal{M}}_{3\pi}|^2(p_+, p_-, p_0)] \\ &\quad - [|\mathcal{M}_{3\pi}|^2(p_-, p_+, p_0) + |\bar{\mathcal{M}}_{3\pi}|^2(p_-, p_+, p_0)] \}, \end{aligned} \quad (40)$$

and noting Eq. (38), we observe that  $\mathcal{A}_{3\pi}$  is odd under  $p_+ \leftrightarrow p_-$  exchange and that it is also manifestly CP odd. Consequently, the observation of a population asymmetry, that is, the failure of mirror symmetry across the Dalitz plot of the untagged decay rate, signals the presence of direct CP violation. To determine the amplitude combinations which give rise to a population asymmetry, let us consider the transformation properties of the amplitudes of Eq. (37) under  $p_+ \leftrightarrow p_-$ , as this is the mirror transformation of the Dalitz plot. We have

$$\mathcal{M}_g^l \xleftrightarrow{p_+ \leftrightarrow p_-} (-1)^l \mathcal{M}_g^l, \quad \mathcal{M}_u^l \xleftrightarrow{p_+ \leftrightarrow p_-} -(-1)^l \bar{\mathcal{M}}_u^l, \quad \mathcal{M}_n^l \xleftrightarrow{p_+ \leftrightarrow p_-} (-1)^l \mathcal{M}_n^l, \quad (41)$$

where analogous relationships hold for the barred amplitudes as well. We thus determine that if  $j + l$  is even only the amplitude combinations

$$\mathcal{M}_g^{j*} \mathcal{M}_u^l + \bar{\mathcal{M}}_g^{j*} \bar{\mathcal{M}}_u^l \quad \text{and} \quad \mathcal{M}_u^{j*} \mathcal{M}_n^l + \bar{\mathcal{M}}_u^{j*} \bar{\mathcal{M}}_n^l, \quad (42)$$

are odd under the mirror symmetry of the Dalitz plot, whereas if  $j + l$  is odd only

$$\begin{aligned} &\mathcal{M}_g^{j*} \mathcal{M}_g^l + \bar{\mathcal{M}}_g^{j*} \bar{\mathcal{M}}_g^l, \\ &\mathcal{M}_u^{j*} \mathcal{M}_u^l + \bar{\mathcal{M}}_u^{j*} \bar{\mathcal{M}}_u^l, \\ &\mathcal{M}_n^{j*} \mathcal{M}_n^l + \bar{\mathcal{M}}_n^{j*} \bar{\mathcal{M}}_n^l, \quad \text{and} \quad \mathcal{M}_g^{j*} \mathcal{M}_n^l + \bar{\mathcal{M}}_g^{j*} \bar{\mathcal{M}}_n^l, \end{aligned} \quad (43)$$

are odd under the mirror symmetry of the Dalitz plot. These amplitude combinations generate a population asymmetry in the tagged decay rate, which we have established as a signal of direct CP violation. As a plurality of amplitude combinations exist, they can act in concert to dilute the population asymmetry we have discussed. Nevertheless, the observation of a population asymmetry in the untagged decay rate to three pseudoscalar mesons is an unambiguous signal of direct CP violation.

Our discussion generalizes the CP-odd amplitudes found under an assumption of  $\rho$  dominance, Eq. (11), in two ways. Firstly, Eq. (42) shows that combinations analogous in structure to Eq. (11) exist for all even  $j + l$ . Equation (43) shows that direct CP violation can also be generated for odd  $j + l$ , such as through  $s$ -wave and  $p$ -wave interference.

### III. COMPARISON TO THE PARTIAL-RATE ASYMMETRY

We wish to compare the size of the population asymmetry in the untagged decay rate with that of the partial rate asymmetry in the same decay channel. We will show that the two asymmetries can be

comparable in size, favoring the study of direct CP-violation in the untagged decay rate on statistical grounds. We begin by considering the amplitude combination  $a_g^* a_u + \bar{a}_g^* \bar{a}_u$ . We can write  $a_{kl}$  of Eq. (1) in terms of its tree and penguin contributions, as per  $\exp(i\beta) a_{kl} \equiv T_{kl} \exp(-i\alpha) + P_{kl}$ , where both  $T_{kl}$  and  $P_{kl}$  are complex, and the weak phases  $\beta$  and  $\gamma$  are given by  $\exp(-i\beta) \equiv V_{tb} V_{td}^*/|V_{tb} V_{td}|$  and  $\exp(i\gamma) = V_{ub}^* V_{ud}/|V_{ub}^* V_{ud}|$ . We take  $V_{kl}$  to be an element of the CKM matrix, and we employ CKM unitarity to write  $\alpha + \beta + \gamma = \pi$ . Noting  $\exp(-i\beta) \bar{a}_{kl} = T_{kl} \exp(i\alpha) + P_{kl}$ , we have

$$\begin{aligned} a_g &= T_g e^{-i\alpha} + P_g, & a_u &= T_u e^{-i\alpha} + P_u, \\ \bar{a}_g &= T_g e^{i\alpha} + P_g, & \bar{a}_u &= -T_u e^{i\alpha} - P_u, \end{aligned} \quad (44)$$

where  $T_g = T_{+-} + T_{-+}$  and  $T_u = T_{+-} - T_{-+}$ , with similar relations for  $P_{g,u}$ . We omit the overall factors of  $\exp(\pm i\beta)$  which ought appear in Eq. (44) as they contribute to neither  $|\mathcal{M}_f|^2$ ,  $|\bar{\mathcal{M}}_f|^2$ , nor  $q\mathcal{M}_f^* \bar{\mathcal{M}}_f/p$  — we note that  $q/p = \exp(-2i\beta)$  in the SM if  $|q/p| = 1$ . With  $r_\kappa \exp(i\delta_\kappa) \equiv P_\kappa/T_\kappa$  for  $\kappa = g, u$ , so that  $r_\kappa = |P_\kappa/T_\kappa|$ , we find [19]

$$a_g a_u^* + \bar{a}_g \bar{a}_u^* = -2 T_g T_u^* \sin \alpha \left[ r_g \sin \delta_g + r_u \sin \delta_u - i(r_g \cos \delta_g - r_u \cos \delta_u) \right]. \quad (45)$$

The decay width associated with this amplitude combination,  $\Gamma_{3\pi}^{(2)}$  in Eq. (7), contains

$$\text{Re} \left[ (a_g a_u^* + \bar{a}_g \bar{a}_u^*) f_g f_u^* \right], \quad (46)$$

so that it is sensitive to both its real and imaginary parts, because the function  $f_g f_u^*$  is also complex — its imaginary part is generated by the non-zero  $\rho$  resonance width. If we assume  $T_g T_u^*$  to be real, for definiteness, and consider the imaginary part of Eq. (45), which accompanies  $\text{Im}(f_g f_u^*)$ , we see that  $\Gamma_{3\pi}^{(2)}$  can be non-zero, so that direct CP violation can exist, even if the strong phases of  $a_i$  were to vanish. Merely  $r_g$  or  $r_u$  must be non-zero, which is easily satisfied. Consequently the observables of Eq. (15) can be non-zero irrespective of the strong phases of  $a_i$  if the width of the resonance in the CP-enantiomer is non-zero. Note that were  $T_g T_u^*$  complex, the  $\rho$  width would not be needed to generate DCPV. Similar considerations exist in  $B \rightarrow V_1 V_2$  decays. There, too, direct CP violation can occur in the untagged decay rate; moreover, its presence does not demand the strong phase of the weak transition amplitude to be non-zero [33].

In contrast, the partial-rate asymmetry associated with  $B^0 \rightarrow \rho^+ \pi^-$  decay is

$$\Gamma_{B^0 \rightarrow \rho^+ \pi^-} - \Gamma_{\bar{B}^0 \rightarrow \rho^- \pi^+} \propto |a_{+-}|^2 - |\bar{a}_{-+}|^2 = -4 |T_{+-}|^2 r_{+-} \sin \delta_{+-} \sin \alpha, \quad (47)$$

so that both  $\alpha$  and  $\delta_{+-}$  must be non-zero to yield a non-zero partial rate asymmetry. Generally one expects  $|\mathcal{M}_{\rho^+ \pi^-}| > |\mathcal{M}_{\rho^- \pi^+}|$  [34–38]; this is borne out by experiment [39]. In the limit where  $\mathcal{M}_{\rho^- \pi^+}$  becomes negligibly small, we see that Eq. (45) becomes

$$a_g a_u^* + \bar{a}_g \bar{a}_u^* \rightarrow -4 |T_{+-}|^2 r_{+-} \sin \delta_{+-} \sin \alpha, \quad (48)$$

so that the population asymmetry of Eq. (15) is identical to the partial rate asymmetry in this limit.

In the following section, we illustrate these ideas numerically and discuss their experimental realization in greater detail. After our analysis of  $B \rightarrow \rho \pi \rightarrow \pi^+ \pi^- \pi^0$  decay, we turn to other modes, studying  $B \rightarrow D^{*\pm} D^\mp \rightarrow D^+ D^- \pi^0$ ,  $B_s \rightarrow K^{*\pm} K^\mp \rightarrow K^+ K^- \pi^0$ , and  $B_s \rightarrow D_s^{*\pm} D_s^\mp \rightarrow D_s^+ D_s^- \pi^0$  decays. We discuss the utility of these modes in realizing tests of the SM.

## IV. NUMERICAL ESTIMATES

In this section we estimate the population asymmetries associated with the untagged decay rate in a variety of decays to self-conjugate final states. We do this for definiteness, though our essential conclusions do not rely on these estimates: the population asymmetry in the untagged decay rate can be of the same numerical size as the partial rate asymmetry in the comparable, tagged decay, making the search for DCPV in the untagged process advantageous.

We begin our numerical analysis by considering the effective, weak Hamiltonian for the decay  $b \rightarrow q q' \bar{q}'$  and its CP-conjugate, where  $q = d, s$  and  $q' = u, d, s, c$ . In the SM, we have [40]

$$\mathcal{H}_{\text{eff}} = \frac{G_F}{\sqrt{2}} \left[ \lambda_u^{(q)} (C_1 Q_1^u + C_2 Q_2^u) + \lambda_c^{(q)} (C_1 Q_1^c + C_2 Q_2^c) - \lambda_t^{(q)} \left( \sum_{i=3}^{10} C_i Q_i + C_{8G} Q_{8G} \right) \right] + \text{H.c.}, \quad (49)$$

where  $G_F$  is the Fermi coupling constant and the factor  $\lambda_{q'}^{(q)} \equiv V_{q'b} V_{q'q}^*$  contains a CKM matrix element  $V_{ij}$ . The Wilson coefficients  $C_i$  are evaluated at the renormalization scale  $\mu$ , and  $Q_{1,\dots,10}$  are four-quark operators, whereas  $Q_{8G}$  is the chromomagnetic penguin operator. The  $C_i$  and  $Q_i$  are detailed in Ref. [40], though we interchange  $C_1 Q_1^q \leftrightarrow C_2 Q_2^q$ , so that  $C_1 \sim 1$  and  $C_1 > |C_2| \gg C_{3,\dots,10,8G}$ . For the CKM matrix elements, we adopt the Wolfenstein parametrization [4],

$$\begin{aligned} V_{ud} &= 1 - \lambda^2/2, & V_{us} &= \lambda, & V_{ub} &= A\lambda^3(\rho - i\eta), \\ V_{cd} &= -\lambda, & V_{cs} &= 1 - \lambda^2/2, & V_{cb} &= A\lambda^2, \\ V_{td} &= A\lambda^3(1 - \rho - i\eta), & V_{ts} &= -A\lambda^2, & V_{tb} &= 1, \end{aligned} \quad (50)$$

neglecting  $\mathcal{O}(\lambda^4)$ , where the parameters are given by [34]

$$\lambda = 0.2205, \quad A = 0.81, \quad \rho = 0.12, \quad \eta = 0.34. \quad (51)$$

The three-body decays we consider proceed from hadronic two-body weak transitions of the form  $B \rightarrow XY$ , for which the amplitude is given by

$$\mathcal{M}_{B \rightarrow XY} = \langle XY | \mathcal{H}_{\text{eff}} | B \rangle. \quad (52)$$

For definiteness and simplicity, we employ the generalized factorization approximation [34, 41], which makes use of next-to-leading-order perturbative-QCD to estimate the needed strong phases. In this approach, the matrix elements  $C_i(\mu) \langle XY | Q_i(\mu) | B \rangle$  are approximated by  $C_i^{\text{eff}} \langle XY | Q_i | B \rangle_{\text{tree}}$ , where the  $C_i^{\text{eff}}$  are effective Wilson coefficients and the  $\langle XY | Q_i | B \rangle_{\text{tree}}$  are calculated under the factorization assumption. The  $C_i^{\text{eff}}$  enter the decay amplitudes through the combinations

$$a_{2i-1} = C_{2i-1}^{\text{eff}} + \frac{C_{2i}^{\text{eff}}}{N_c}, \quad a_{2i} = C_{2i}^{\text{eff}} + \frac{C_{2i-1}^{\text{eff}}}{N_c}, \quad (53)$$

where  $i = 1, \dots, 5$  and  $N_c = 3$ . We adopt the  $a_i$  values at  $\mu = 2.5 \text{ GeV}$  calculated in Ref. [34], collected in their Tables VI and VII. For reference, we report these numbers in Table III in the Appendix. Our purpose is to gain an impression of the relative size of the partial rate and population asymmetries in a variety of modes.

### A. $B \rightarrow \pi^+ \pi^- \pi^0$

We now evaluate the CP-odd observables in untagged  $B^0, \bar{B}^0 \rightarrow \pi^+ \pi^- \pi^0$  decays. To begin, we assume, as in Sec. II, that  $B^0, \bar{B}^0 \rightarrow \pi^+ \pi^- \pi^0$  decays are dominated by  $\rho\pi$  intermediate states. The  $B \rightarrow \rho\pi$  amplitudes we employ, as well as our ancillary input parameters and form factors, are given in the Appendix. The population asymmetries of Eq. (15) are computed using Eqs. (6,7). We begin by computing

$$\Gamma_{ij} \equiv \int d\Phi f_i^* f_j , \quad (54)$$

to find

$$\begin{aligned} \Gamma_{gu}[s_{+0} > s_{-0}] &= -\Gamma_{gu}[s_{+0} < s_{-0}] = (-54.57 - 3.05i) \times 10^{10} \Gamma_{B^0} , \\ \Gamma_{un}[s_{+0} > s_{-0}] &= -\Gamma_{un}[s_{+0} < s_{-0}] = (2.01 - 0.08i) \times 10^{10} \Gamma_{B^0} , \end{aligned} \quad (55)$$

where the arguments in brackets indicate the regions in phase space over which the integral is calculated. The bracketed regions can also be selected by fixing the sign of  $\cos\theta$ , where  $\theta$  is the helicity angle. We define  $\theta$  in  $B(p_B) \rightarrow \pi^+(p_+) \pi^-(p_-) \pi^0(p_0)$  decay via

$$\cos\theta = \frac{\mathbf{p}'_- \cdot \mathbf{p}'_0}{|\mathbf{p}'_-| |\mathbf{p}'_0|} , \quad (56)$$

where the primed variables refer to the momenta in the rest frame of the  $\pi^+(p'_+) \pi^-(p'_-)$  pair, so that  $\mathbf{p}'_+ + \mathbf{p}'_- = 0$ . Note that  $s_{-0} \leq s_{+0}$  corresponds to  $\cos\theta \leq 0$ . The Im parts of  $\Gamma_{gu}$  and  $\Gamma_{un}$  are relatively small, so that short-distance strong phases are necessary, from a practical viewpoint, to observe a population asymmetry. Employing the model of Ref. [34] and the parameters reported in the Appendix, we find

$$a_g^* a_u + \bar{a}_g^* \bar{a}_u = (0.616 - 1.683i) \times 10^{-18} , \quad a_u^* a_n + \bar{a}_u^* \bar{a}_n = (0.186 - 0.664i) \times 10^{-18} . \quad (57)$$

It is useful to report the separate  $\Gamma^{(i)}$  contributions to the asymmetries, as per Eqs. (6,7), as well. To this end, we define

$$\mathcal{B}^{(i)} \equiv \frac{\Gamma_{B \rightarrow 3\pi}^{(i)}[s_{+0} > s_{-0}]}{\Gamma_{B^0}} , \quad \mathcal{B}_{3\pi} \equiv \frac{\Gamma(B^0, \bar{B}^0 \rightarrow \pi^+ \pi^- \pi^0)}{\Gamma_{B^0}} , \quad (58)$$

so that Eq. (15) can be rewritten

$$\mathcal{A}_{3\pi}^{(i)} = \frac{2\mathcal{B}^{(i)}}{\mathcal{B}_{3\pi}} . \quad (59)$$

We have

$$\begin{aligned} \mathcal{B}_{3\pi}^{(2)}[s_{+0} > s_{-0}] &= -7.8 \times 10^{-7} , & \mathcal{B}_{3\pi}^{(3)}[s_{+0} > s_{-0}] &= +6.4 \times 10^{-9} , \\ \mathcal{B}_{3\pi} &= 2\mathcal{B}_{3\pi}^{(1)}[s_{+0} > s_{-0}] = 46 \times 10^{-6} , \end{aligned} \quad (60)$$

to yield

$$\mathcal{A}_{3\pi}^{(2)} = -3.4\% , \quad \mathcal{A}_{3\pi}^{(3)} = 0.03\% . \quad (61)$$

The CP-violating asymmetry of Eq. (14) is thus

$$\mathcal{A}_{3\pi} = -3.3\% , \quad (62)$$

which is clearly dominated by  $\mathcal{A}_{3\pi}^{(2)}$ , the  $\Gamma_{3\pi}^{(2)}$  contribution. This is expected because  $\Gamma_{3\pi}^{(3)}$  contains, in comparison, the  $B(\bar{B}) \rightarrow \rho^0 \pi^0$  amplitude, which is “color-suppressed” at tree-level; it is also suppressed by phase space, as per Eq. (55).

In constructing the population asymmetry, we need not integrate over the entire, allowed region. We can also study the population asymmetry over regions of the Dalitz plot; this is realized in Table I. Selecting the regions where the  $\rho$  bands overlap enhances the population asymmetry, but to the detriment of its detectability, as the branching ratio into the selected regions of the Dalitz plot,  $\mathcal{B}_{3\pi}$ , becomes considerably smaller. Indeed, for a direct CP search it would be more efficacious to use the entire allowed region.

TABLE I: The ratios  $\mathcal{B}^{(i)} \equiv \mathcal{B}_{3\pi}^{(i)}[s_{+0} > s_{-0}] = \Gamma_{3\pi}^{(i)}[s_{+0} > s_{-0}] / \Gamma_{B^0}$  for  $i = 2, 3$ , total branching-ratio  $\mathcal{B}_{3\pi} = \Gamma_{3\pi} / \Gamma_{B^0}$ , and population asymmetry  $\mathcal{A}_{3\pi}$ , corresponding to various integration regions within the Dalitz plot, with  $m_{kl} = \sqrt{s_{kl}}$ . The  $\mathcal{B}_{3\pi}$  entries includes contributions from both sides of the  $s_{+0} = s_{-0}$  line.

Region within Dalitz plot	$\mathcal{B}^{(2)}$	$\mathcal{B}^{(3)}$	$\mathcal{B}_{3\pi}$	$\mathcal{A}_{3\pi} = \frac{2\mathcal{B}^{(2)} + 2\mathcal{B}^{(3)}}{\mathcal{B}_{3\pi}} (\%)$
entire allowed region	$-7.8 \times 10^{-7}$	$+6.4 \times 10^{-9}$	$46 \times 10^{-6}$	-3.3
$m_\rho - 3\Gamma_\rho < m_{+0}, m_{-0} < m_\rho + 3\Gamma_\rho$	$-6.6 \times 10^{-8}$	$-4 \times 10^{-12}$	$22 \times 10^{-7}$	-6.1
$m_\rho - 2\Gamma_\rho < m_{+0}, m_{-0} < m_\rho + 2\Gamma_\rho$	$-2.8 \times 10^{-8}$	$-1 \times 10^{-12}$	$73 \times 10^{-8}$	-7.6
$m_\rho - \Gamma_\rho < m_{+0}, m_{-0} < m_\rho + \Gamma_\rho$	$-1.4 \times 10^{-9}$	$-4 \times 10^{-14}$	$31 \times 10^{-9}$	-9.3
$m_\rho - 3\Gamma_\rho < m_{+-}, m_{-0} < m_\rho + 3\Gamma_\rho$	$-3.8 \times 10^{-8}$	$+0.4 \times 10^{-8}$	$27 \times 10^{-7}$	-2.6
$m_\rho - 2\Gamma_\rho < m_{+-}, m_{-0} < m_\rho + 2\Gamma_\rho$	$-1.5 \times 10^{-8}$	$+0.2 \times 10^{-8}$	$10 \times 10^{-7}$	-2.3
$m_\rho - \Gamma_\rho < m_{+-}, m_{-0} < m_\rho + \Gamma_\rho$	$-1.0 \times 10^{-9}$	$+0.3 \times 10^{-9}$	$76 \times 10^{-9}$	-1.9

More realistically,  $B \rightarrow 3\pi$  decays will contain contributions from other than  $B \rightarrow \rho^i \pi^j \rightarrow 3\pi$ . We can isolate the individual  $\Gamma_{3\pi}^{(2,3)}$  contributions by restricting the integration regions to the  $\rho$  bands, which lie close to the edges of the Dalitz plot, as shown in Fig. 1. To realize this, we integrate over the region of  $3\pi$  phase-space satisfying the requirement that the invariant mass of two of the three pions yield the  $\rho$  mass within an interval of  $M_\rho \pm \delta$ . This amounts to calculating the effective width

$$\Gamma_{B \rightarrow \rho(p_1+p_2)\pi(p_3)}^{\text{eff}} = \Gamma(B \rightarrow \pi(p_1)\pi(p_2)\pi(p_3)) \Big|_{(M_\rho - \delta)^2 \leq s_{12} \leq (M_\rho + \delta)^2} . \quad (63)$$

In an experimental analysis the strength associated with the complete  $\rho$  line shape would be assessed; our effective width Ansatz is a simple simulcrum of this more sophisticated analysis. In order to

avoid double counting in determining the population asymmetries, we further require that the  $\rho^-\pi^+$  ( $\rho^+\pi^-$ ) contributions be restricted to the  $s_{+0} > s_{-0}$  ( $s_{+0} < s_{-0}$ ) region. The resulting effective branching ratios for  $\delta = 0.3 \text{ GeV}$  are

$$\begin{aligned} \mathcal{B}_{B^0 \rightarrow \rho^-\pi^+}^{\text{eff}}[s_{+0} > s_{-0}] &= 4.9 \times 10^{-6}, & \mathcal{B}_{B^0 \rightarrow \rho^+\pi^-}^{\text{eff}}[s_{+0} < s_{-0}] &= 17.6 \times 10^{-6}, \\ \mathcal{B}_{\bar{B}^0 \rightarrow \rho^-\pi^+}^{\text{eff}}[s_{+0} > s_{-0}] &= 16.2 \times 10^{-6}, & \mathcal{B}_{\bar{B}^0 \rightarrow \rho^+\pi^-}^{\text{eff}}[s_{+0} < s_{-0}] &= 4.9 \times 10^{-6}, \end{aligned} \quad (64)$$

and

$$\begin{aligned} \mathcal{B}_{B^0 \rightarrow \rho^0\pi^0}^{\text{eff}}[s_{+0} > s_{-0}] &= 0.18 \times 10^{-6}, & \mathcal{B}_{B^0 \rightarrow \rho^0\pi^0}^{\text{eff}}[s_{+0} < s_{-0}] &= 0.56 \times 10^{-6}, \\ \mathcal{B}_{\bar{B}^0 \rightarrow \rho^0\pi^0}^{\text{eff}}[s_{+0} > s_{-0}] &= 0.48 \times 10^{-6}, & \mathcal{B}_{\bar{B}^0 \rightarrow \rho^0\pi^0}^{\text{eff}}[s_{+0} < s_{-0}] &= 0.16 \times 10^{-6}. \end{aligned} \quad (65)$$

For reference, we report the two-body branching ratios and the corresponding rate asymmetries of the decay modes considered in this paper in Table II. We note that the combined branching ratios of the two-body  $B \rightarrow \rho^\pm\pi^\mp$  branching ratios we report are slightly high with respect to recent measurements [42–44], but the estimates would be consistent with the data if the uncertainties in the input parameters were taken into account. Returning to our discussion, we find that the effective  $\rho^0\pi^0$  branching ratios are much enhanced with respect to the corresponding two-body rates in Table II — this is caused by the large interference with the  $\rho^\pm\pi^\mp$  contributions. The population asymmetries about the  $s_{+0} = s_{-0}$  line are then

$$\begin{aligned} \mathcal{A}_{3\pi}^{+-} &\equiv \frac{\Gamma_{B,\bar{B} \rightarrow \rho^-\pi^+}^{\text{eff}}[s_{+0} > s_{-0}] - \Gamma_{B,\bar{B} \rightarrow \rho^+\pi^-}^{\text{eff}}[s_{+0} < s_{-0}]}{\Gamma_{B,\bar{B} \rightarrow \rho^-\pi^+}^{\text{eff}}[s_{+0} > s_{-0}] + \Gamma_{B,\bar{B} \rightarrow \rho^+\pi^-}^{\text{eff}}[s_{+0} < s_{-0}]} = -3.3\%, \\ \mathcal{A}_{3\pi}^{00} &\equiv \frac{\Gamma_{B,\bar{B} \rightarrow \rho^0\pi^0}^{\text{eff}}[s_{+0} > s_{-0}] - \Gamma_{B,\bar{B} \rightarrow \rho^0\pi^0}^{\text{eff}}[s_{+0} < s_{-0}]}{\Gamma_{B,\bar{B} \rightarrow \rho^0\pi^0}^{\text{eff}}[s_{+0} > s_{-0}] + \Gamma_{B,\bar{B} \rightarrow \rho^0\pi^0}^{\text{eff}}[s_{+0} < s_{-0}]} = -4.6\%, \end{aligned} \quad (66)$$

to be compared with  $\mathcal{A}_{3\pi}^{(2)}, \mathcal{A}_{3\pi}^{(3)}$ , respectively, in Eq. (61). There is very little  $\Gamma_{3\pi}^{(3)}$  contribution in  $\mathcal{A}_{3\pi}^{+-}$ , whereas in  $\mathcal{A}_{3\pi}^{00}$  the  $\Gamma_{3\pi}^{(2)}$  dominance is much less pronounced, yielding  $\sim -2.6$  in the  $-4.6$ . Practically, it is challenging to measure  $\mathcal{A}_{3\pi}^{00}$ , due to the smallness of the effective  $\rho^0\pi^0$  rates. We note that the numerical value of  $\mathcal{A}_{3\pi}^{+-}$  is fairly close to that of  $\mathcal{A}_{CP}$  for  $B^0 \rightarrow \rho^+\pi^-$  in Table II, and this arises from the dominance of the  $B^0 \rightarrow \rho^+\pi^-$  and  $\bar{B}^0 \rightarrow \rho^-\pi^+$  contributions in the  $\rho^\pm$  regions of the Dalitz plot.

We expect that  $B, \bar{B} \rightarrow \pi^+\pi^-\pi^0$  decay is not populated exclusively by  $B, \bar{B} \rightarrow \rho\pi$  contributions; other resonant and nonresonant contributions ought occur — and can potentially enter the  $\rho\pi$  phase space as well. Among the latter, contributions mediated by the  $B^*$  meson may be important [46, 47]. Such effects are expected, however, to be suppressed by the  $BB^*\pi$  vertex, as the  $B^*$  is highly off-mass-shell in the relevant kinematical region [48], so that we shall not consider these effects further. As for contributions from other resonances, we expect the “ $\sigma$ ,” or  $f_0(400 - 1200)$ , a broad isospin  $I = 0$  and spin  $J = 0$  enhancement in  $\pi\pi$  scattering, to play a modest role [47–49]. The peak of this enhancement is close to the  $\rho$  in mass, and the  $\sigma\pi^0$  intermediate state contributes preferentially to the  $\rho^0\pi^0$  phase space. To explore how corrections to  $\rho$  “dominance” can impact the population asymmetry, we assume that the  $\sigma$  resonance is the only additional contribution to the  $3\pi$  final states, in the  $\rho$  bands on the Dalitz plot.

TABLE II: Estimated two-body branching ratios and rate asymmetries using the model of Ref. [34] and the input parameters given in the Appendix.

Decay mode $B \rightarrow VP$	$10^6 \mathcal{B}_{B \rightarrow VP}$	$10^6 \mathcal{B}_{\bar{B} \rightarrow \bar{V}\bar{P}}$	$\mathcal{A}_{CP} = \frac{\Gamma_{\bar{B} \rightarrow \bar{V}\bar{P}} - \Gamma_{B \rightarrow VP}}{\Gamma_{\bar{B} \rightarrow \bar{V}\bar{P}} + \Gamma_{B \rightarrow VP}} (\%)$
$B^0 \rightarrow \rho^+ \pi^-$	23.2	21.4	-4.1
$B^0 \rightarrow \rho^- \pi^+$	6.47	6.30	-1.3
$B^0 \rightarrow \rho^0 \pi^0$	0.047	0.068	19
$B^0 \rightarrow D^{*+} D^-$	376	384	1.0
$B^0 \rightarrow D^{*-} D^+$	322	323	0.3
$B_s^0 \rightarrow K^{*+} K^-$	3.44	4.76	16
$B_s^0 \rightarrow K^{*-} K^+$	0.271	0.375	16
$B_s^0 \rightarrow D_s^{*+} D_s^-$	10044	10028	-0.08
$B_s^0 \rightarrow D_s^{*-} D_s^+$	8628	8623	-0.03

We express the  $B \rightarrow \sigma\pi^0$  amplitudes as

$$\mathcal{M}_{B^0 \rightarrow \pi^0 \sigma} = a_\sigma, \quad \mathcal{M}_{\bar{B}^0 \rightarrow \pi^0 \sigma} = \bar{a}_\sigma. \quad (67)$$

In the presence of the  $\sigma$ , the  $B \rightarrow 3\pi$  amplitudes in Eq. (2) become

$$\mathcal{M}_{3\pi} = a_g f_g + a_u f_u + a_n f_n + a_\sigma f_\sigma, \quad \bar{\mathcal{M}}_{3\pi} = \bar{a}_g f_g + \bar{a}_u f_u + \bar{a}_n f_n + \bar{a}_\sigma f_\sigma, \quad (68)$$

where  $f_\sigma$  is the form factor describing the  $\sigma \rightarrow \pi^+ \pi^-$  transition. Expressions for the  $B \rightarrow \sigma\pi$  amplitudes and  $f_\sigma$  are given in the Appendix. The resulting  $B \rightarrow 3\pi$  width is

$$\begin{aligned} \Gamma_{3\pi} = & \int d\Phi \left\{ \sum_{\kappa=g,u,n,\sigma} \left( |a_\kappa|^2 + |\bar{a}_\kappa|^2 \right) |f_\kappa|^2 + 2 \text{Re} \left[ (a_g^* a_n + \bar{a}_g^* \bar{a}_n) f_g^* f_n + (a_u^* a_\sigma + \bar{a}_u^* \bar{a}_\sigma) f_u^* f_\sigma \right] \right\} \\ & + \Gamma_{3\pi}^{(2)} + \Gamma_{3\pi}^{(3)} + \Gamma_{3\pi}^{(4)} + \Gamma_{3\pi}^{(5)}, \end{aligned} \quad (69)$$

where  $\Gamma_{3\pi}^{(2,3)}$  are given in (7) and

$$\Gamma_{3\pi}^{(4)} = \int d\Phi 2 \text{Re} \left[ (a_g^* a_\sigma + \bar{a}_g^* \bar{a}_\sigma) f_g^* f_\sigma \right], \quad \Gamma_{3\pi}^{(5)} = \int d\Phi 2 \text{Re} \left[ (a_n^* a_\sigma + \bar{a}_n^* \bar{a}_\sigma) f_n^* f_\sigma \right]. \quad (70)$$

With the inclusion of the  $\sigma$ , we encounter more CP-violating observables. Under CP transformations we also have<sup>7</sup>

$$a_\sigma \xleftrightarrow{CP} -\bar{a}_\sigma, \quad (71)$$

<sup>7</sup> Noting  $CP|\sigma\rangle = +|\sigma\rangle$ , we find  $\langle \pi^0(p_0)\sigma(p_\sigma)|Q_i|\bar{B}^0\rangle = -\eta_B^* \eta_Q \langle \pi^0(p_0)\sigma(p_\sigma)|Q_i^\dagger|B^0\rangle$  where  $p_\sigma = p_+ + p_-$  and  $\mathbf{p}_\sigma = \mathbf{0}$ . With  $\eta_B^* \eta_Q = +1$ , we recover Eq. (71).

so that  $a_u^* a_\sigma + \bar{a}_u^* \bar{a}_\sigma$  in Eq. (69) is CP even, whereas

$$a_g^* a_\sigma + \bar{a}_g^* \bar{a}_\sigma \quad \text{and} \quad a_n^* a_\sigma + \bar{a}_n^* \bar{a}_\sigma \quad (72)$$

in Eq. (70) are CP odd, the latter serving as specific examples of the CP-violating amplitudes given in Eq. (43). As we have discussed in conjunction with Eq. (11), a nonzero value of any one of the last two combinations signals direct CP violation. Noting that  $f_\sigma$  is even under the interchange  $s_{+0} \leftrightarrow s_{-0}$ , we can see that both  $f_g^* f_\sigma$  and  $f_n^* f_\sigma$  are odd under such an interchange. It follows that

$$\Gamma_{3\pi}^{(4,5)}[s_{+0} > s_{-0}] = -\Gamma_{3\pi}^{(4,5)}[s_{+0} < s_{-0}] , \quad (73)$$

so that  $\Gamma_{3\pi}^{(4,5)}$  contribute to the population asymmetry on the Dalitz plot about the  $s_{+0} = s_{-0}$  line, reflecting direct CP violation, as we have discussed in Sec. II. We remark that the CP-odd observables in Eq. (72) share with those in Eq. (11) the unusual property that they do not rely on the nonvanishing of the strong phases in  $a_i$ . However, the combinations in Eq. (72) arise not from the interference of a pair of CP-conjugate states yielding the ones in Eq. (11), but from the interference of the  $\rho^0 \pi^0$  and  $\sigma \pi^0$  intermediate states which have different relative angular-momenta,  $l = 1$  and 0, respectively.

To find the asymmetries in the presence of the  $\sigma$ , we recompute the effective branching ratios for  $\delta = 0.3$  GeV, as reported in Eqs. (64) and (65). The results are

$$\begin{aligned} \mathcal{B}_{B^0 \rightarrow \rho^- \pi^+}^{\text{eff}}[s_{+0} > s_{-0}] &= 4.8 \times 10^{-6} , & \mathcal{B}_{B^0 \rightarrow \rho^+ \pi^-}^{\text{eff}}[s_{+0} < s_{-0}] &= 17.6 \times 10^{-6} , \\ \mathcal{B}_{\bar{B}^0 \rightarrow \rho^- \pi^+}^{\text{eff}}[s_{+0} > s_{-0}] &= 16.2 \times 10^{-6} , & \mathcal{B}_{\bar{B}^0 \rightarrow \rho^+ \pi^-}^{\text{eff}}[s_{+0} < s_{-0}] &= 4.8 \times 10^{-6} , \end{aligned} \quad (74)$$

$$\begin{aligned} \mathcal{B}_{B^0 \rightarrow \rho^0 \pi^0}^{\text{eff}}[s_{+0} > s_{-0}] &= 0.18 \times 10^{-6} , & \mathcal{B}_{B^0 \rightarrow \rho^0 \pi^0}^{\text{eff}}[s_{+0} < s_{-0}] &= 0.58 \times 10^{-6} , \\ \mathcal{B}_{\bar{B}^0 \rightarrow \rho^0 \pi^0}^{\text{eff}}[s_{+0} > s_{-0}] &= 0.51 \times 10^{-6} , & \mathcal{B}_{\bar{B}^0 \rightarrow \rho^0 \pi^0}^{\text{eff}}[s_{+0} < s_{-0}] &= 0.16 \times 10^{-6} , \end{aligned} \quad (75)$$

which indicate that the effects of the  $\sigma$  in the  $\rho^\pm \pi^\mp$  bands are really very small. The population asymmetries about the  $s_{+0} = s_{-0}$  line are then

$$\begin{aligned} \mathcal{A}_{3\pi}^{+-} &= \frac{\Gamma_{B, \bar{B} \rightarrow \rho^- \pi^+}^{\text{eff}}[s_{+0} > s_{-0}] - \Gamma_{B, \bar{B} \rightarrow \rho^+ \pi^-}^{\text{eff}}[s_{+0} < s_{-0}]}{\Gamma_{B, \bar{B} \rightarrow \rho^- \pi^+}^{\text{eff}}[s_{+0} > s_{-0}] + \Gamma_{B, \bar{B} \rightarrow \rho^+ \pi^-}^{\text{eff}}[s_{+0} < s_{-0}]} = -3.3\% , \\ \mathcal{A}_{3\pi}^{00} &= \frac{\Gamma_{B, \bar{B} \rightarrow \rho^0 \pi^0}^{\text{eff}}[s_{+0} > s_{-0}] - \Gamma_{B, \bar{B} \rightarrow \rho^0 \pi^0}^{\text{eff}}[s_{+0} < s_{-0}]}{\Gamma_{B, \bar{B} \rightarrow \rho^0 \pi^0}^{\text{eff}}[s_{+0} > s_{-0}] + \Gamma_{B, \bar{B} \rightarrow \rho^0 \pi^0}^{\text{eff}}[s_{+0} < s_{-0}]} = -3.0\% . \end{aligned} \quad (76)$$

Comparing the  $\mathcal{A}_{3\pi}^{+-}$  values in Eqs. (66) and (76) with  $\mathcal{A}_{3\pi}$  in Eq. (62), we see that  $\mathcal{A}_{3\pi}^{+-}$  captures the CP-violating effects occurring in the dominant  $\rho^\pm \pi^\mp$  modes, as encoded in  $\Gamma_{3\pi}^{(2)}$ . In contrast, the  $\mathcal{A}_{3\pi}^{00}$  value in Eq. (76) receives the respective contributions  $(-2.6 - 2.0 + 1.9 - 0.3)\%$  from  $\Gamma_{3\pi}^{(2+3+4+5)}$ , so that the presence of the  $\sigma$  leads to a sizable reduction of the asymmetry. The interpretation of this latter asymmetry is thus rendered more difficult.

The untagged asymmetry, in specific,  $\mathcal{A}_{3\pi}^{+-}$ , has been investigated by BaBar and Belle. BaBar reports [43]

$$\mathcal{A}_{CP}^{\rho\pi} = \frac{\Gamma_{B, \bar{B} \rightarrow \rho^+ \pi^-}^{\text{eff}} - \Gamma_{B, \bar{B} \rightarrow \rho^- \pi^+}^{\text{eff}}}{\Gamma_{B, \bar{B} \rightarrow \rho^- \pi^+}^{\text{eff}} + \Gamma_{B, \bar{B} \rightarrow \rho^+ \pi^-}^{\text{eff}}} = -0.18 \pm 0.08 \pm 0.03 , \quad (77)$$

with the recent update  $\mathcal{A}_{CP}^{\rho\pi} = -0.11 \pm 0.06 \pm 0.03$  [45]. The  $s_{+0} \gtrless s_{-0}$  criterion we impose in Eq. (66) has apparently not been effected in  $\mathcal{A}_{CP}^{\rho\pi}$ . Thus this quantity may well treat events in the region where the  $\rho^\pm$  bands overlap inappropriately. In the theoretical analysis we report in Table I, the impact of the overlap region, which contains an intrinsically larger asymmetry, is diluted by its small contribution to the total  $B \rightarrow \rho^\pm \pi^\mp$  decay rate. Thus the  $s_{+0} \gtrless s_{-0}$  correction may not be essential;  $\mathcal{A}_{CP}^{\rho\pi}$  may well be tantamount to  $-\mathcal{A}_{3\pi}^{+-}$ . The Belle measurement, in contrast, removes events with an ambiguous  $\rho$  charge assignment from their data set [44]; this is a practical realization of our  $s_{+0} \gtrless s_{-0}$  criterion. Belle reports [44]

$$\mathcal{A} = -0.38_{-0.21}^{+0.19}(\text{stat})_{-0.05}^{+0.04}(\text{syst}), \quad (78)$$

where  $\mathcal{A} = -\mathcal{A}_{3\pi}^{+-}$ .

The central values of the BaBar and Belle measurements, albeit their still-sizeable errors, point to much larger CP-violating effects than what we have calculated. Interestingly, more sophisticated calculations show similar trends. For example,  $A_{3\pi}^{+-}$  has been calculated in the QCD factorization approach to yield the “default results” [38]

$$A_{3\pi}^{+-} = -0.01_{-0.00}^{+0.00+0.01+0.00+0.10}, \quad (79)$$

where larger, more positive asymmetries, outside the stated error ranges, can occur in various excursions from their default assumptions [38]. Here there is no subtlety concerning the “overlap regions” as their assay assumes the  $\rho$  meson has zero-width. Using the results of Table II, we find in comparision that  $A_{3\pi}^{+-} = -0.028$  in this limit, so that our numerical results are of comparable size. Moreover, the size of the partial-rate asymmetry in the  $B \rightarrow \rho^+ \pi^-$  mode is crudely commensurate with the size of  $A_{3\pi}^{+-}$  [38], as we have found in our calculation, so that one would expect that a search for DCPV in these modes through the population asymmetry would be statistically more efficacious.

This concludes our discussion of  $B \rightarrow \pi^+ \pi^- \pi^0$  decay. In what follows we consider how the study of the population asymmetry in other modes can complement tests of the SM and searches for emergent, new phenomena. For example, the time-dependent asymmetry associated with the decay of a state tagged as  $B^0$  or  $\bar{B}^0$  into a CP eigenstate  $f$  is characterized by two parameters:  $C_f$  and  $S_f$ . The first term is generated through direct CP violation, whereas the second is generated through the interference of  $B - \bar{B}$  mixing and direct decay. In the SM  $S_f$  measures  $-\eta_f \sin(2\beta)$ , where  $\eta = +1$  ( $-1$ ) for a CP-even (odd) final state<sup>8</sup>, in modes driven by quark-level transitions such as  $b \rightarrow c\bar{s}$ ,  $b \rightarrow s\bar{s}$ , and  $b \rightarrow c\bar{c}d$ , modulo small corrections [50]. The determination of  $\sin(2\beta)$  from  $S_{J/\psi K_S}$  serves as a benchmark against which  $S_f$ , from other modes, can be measured. The modes  $B \rightarrow \phi K_S$ ,  $B \rightarrow K_S K^+ K^-$  decay, mediated via  $b \rightarrow s\bar{s}$ ,  $B \rightarrow D^{*+} D^-$  decay, mediated via  $b \rightarrow c\bar{c}d$ , and  $B \rightarrow D_s^{*+} D_s^-$  decay, mediated via  $b \rightarrow c\bar{s}$ , serve as examples. Of these, only  $\phi K_S$  is a CP-eigenstate. One can, nevertheless, determine  $S_f$  from the three-body decays, of which the vector-pseudoscalar modes are part; in these cases the coefficient of the  $\sin(\Delta M t)$  term must be corrected for a non-CP-violating dilution factor to yield  $S_f$  [23, 51–53]. We focus on the three-body

<sup>8</sup> We define the asymmetry as  $A(t) \equiv (\Gamma(\bar{B}^0 \rightarrow f) - \Gamma(B^0 \rightarrow f)) / (\Gamma(\bar{B}^0 \rightarrow f) + \Gamma(B^0 \rightarrow f)) \equiv -C_f \cos(\Delta M t) + S_f \sin(\Delta M t)$ .

decays as the population asymmetry therein allows us to test the extent to which the corrections to the SM tests suggested in Ref. [50] really are small. Alternatively, such observables may well help us establish the character of the new physics which induce deviations from the SM predictions. In the following we consider  $B \rightarrow D^{*+}D^- \rightarrow D^+D^-\pi^0$   $B_s \rightarrow D_s^{*+}D_s^- \rightarrow D_s^+D_s^-\pi^0$  decays as an explicit realization of these ideas; we also include  $B_s \rightarrow K^{*+}K^- \rightarrow K^+K^-\pi^0$  decays as well to show that the population asymmetry can also be quite large in the SM.

Before turning to these examples, we note that the population asymmetry may well serve as a useful tool in the study of  $B \rightarrow K_SK^+K^-$  decay. At issue is the extent to which  $B \rightarrow K_SK^+K^-$  decay is CP-even once the regions associated with the  $\phi$  resonance are explicitly removed from consideration [54–56]. We note as per Refs. [55, 56] that the CP-even and CP-odd contributions to  $B \rightarrow [K^+K^-]_l(K_S)_l$  decay differ in their angular momentum character; their interference can give rise to a direct CP-violating population asymmetry as described in Eq. (43). The population asymmetry serves as an independent empirical assay of the reliability of the underlying assumptions of their analysis [54–56].

## B. $B \rightarrow D^+D^-\pi^0$

We write the amplitudes for  $B^0, \bar{B}^0 \rightarrow D^{*+}D^-, D^{*-}D^+$  as

$$\mathcal{M}_{B^0 \rightarrow D^{*k}D^l} = a_{kl} \varepsilon_{D^*}^* \cdot p_D, \quad \mathcal{M}_{\bar{B}^0 \rightarrow D^{*k}D^l} = \bar{a}_{kl} \varepsilon_{D^*}^* \cdot p_D, \quad (80)$$

where the expressions for  $a_{kl}$  and  $\bar{a}_{kl}$  are given in the Appendix. The amplitudes for  $B^0, \bar{B}^0 \rightarrow D^+(p_+) D^-(p_-) \pi^0(p_0)$  are then

$$\begin{aligned} \mathcal{M}_{D\bar{D}\pi} &= a_{+-} f_+ + a_{-+} f_- = a_g f_g + a_u f_u, \\ \bar{\mathcal{M}}_{D\bar{D}\pi} &= \bar{a}_{+-} f_+ + \bar{a}_{-+} f_- = \bar{a}_g f_g + \bar{a}_u f_u. \end{aligned} \quad (81)$$

Here, as in the  $3\pi$  case,

$$\begin{aligned} a_g &= a_{+-} + a_{-+}, & a_u &= a_{+-} - a_{-+}, & \bar{a}_g &= \bar{a}_{+-} + \bar{a}_{-+}, & \bar{a}_u &= \bar{a}_{+-} - \bar{a}_{-+}, \\ 2f_g &= f_+ + f_-, & 2f_u &= f_+ - f_-, \end{aligned} \quad (82)$$

in this case, however, the  $f_\pm$  are given by Eq. (110) in the Appendix. The  $B^0, \bar{B}^0 \rightarrow D^+D^-\pi^0$  amplitudes lead to the decay width

$$\Gamma_{D\bar{D}\pi} = \int d\Phi \left( |\mathcal{M}_{D\bar{D}\pi}|^2 + |\bar{\mathcal{M}}_{D\bar{D}\pi}|^2 \right) = \Gamma_{D\bar{D}\pi}^{(1)} + \Gamma_{D\bar{D}\pi}^{(2)}, \quad (83)$$

where

$$\Gamma_{D\bar{D}\pi}^{(1)} = \int d\Phi \sum_{\kappa=g,u} \left( |a_\kappa|^2 + |\bar{a}_\kappa|^2 \right) |f_\kappa|^2, \quad \Gamma_{D\bar{D}\pi}^{(2)} = \int d\Phi 2 \operatorname{Re} \left[ (a_g^* a_u + \bar{a}_g^* \bar{a}_u) f_g^* f_u \right]. \quad (84)$$

It follows that

$$\Gamma_{D\bar{D}\pi}^{(1)}[s_{+0} > s_{-0}] = +\Gamma_{D\bar{D}\pi}^{(1)}[s_{+0} < s_{-0}], \quad \Gamma_{D\bar{D}\pi}^{(2)}[s_{+0} > s_{-0}] = -\Gamma_{D\bar{D}\pi}^{(2)}[s_{+0} < s_{-0}]. \quad (85)$$

The CP-odd combination  $a_g^* a_u + \bar{a}_g^* \bar{a}_u$  in this case is proportional to  $\sin \beta$ , as can be inferred from the CKM factors in the  $B \rightarrow D^{*\pm} D^\mp$  amplitudes given in the Appendix.

To evaluate  $\Gamma_{D\bar{D}\pi}^{(1,2)}$ , we consider the Dalitz plot of  $s_{+0}$  vs.  $s_{-0}$  for the  $D^+ D^- \pi^0$  final states. Integrating over the two regions divided by the  $s_{+0} = s_{-0}$  line, we find

$$\mathcal{B}_{D\bar{D}\pi}^{(2)}[s_{+0} > s_{-0}] = 1.0 \times 10^{-6}, \quad \mathcal{B}_{D\bar{D}\pi} = 2 \mathcal{B}_{D\bar{D}\pi}^{(1)}[s_{+0} > s_{-0}] = 4.8 \times 10^{-4}, \quad (86)$$

where  $\mathcal{B}_{D\bar{D}\pi}^{(i)} \equiv \Gamma_{D\bar{D}\pi}^{(i)} / \Gamma_{B^0}$  for  $i = 1, 2$ . The resulting CP-violating asymmetry is

$$\mathcal{A}_{D\bar{D}\pi} = \frac{\Gamma_{D\bar{D}\pi}[s_{+0} > s_{-0}] - \Gamma_{D\bar{D}\pi}[s_{+0} < s_{-0}]}{\Gamma_{D\bar{D}\pi}[s_{+0} > s_{-0}] + \Gamma_{D\bar{D}\pi}[s_{+0} < s_{-0}]} = \frac{\Gamma_{D\bar{D}\pi}^{(2)}[s_{+0} > s_{-0}]}{\Gamma_{D\bar{D}\pi}^{(1)}[s_{+0} > s_{-0}]} = +0.4\%. \quad (87)$$

More realistically, the  $D^+ D^- \pi^0$  final states also receive contributions from heavier charmed resonances such as the  $D_0$  and  $D_2$  mesons [57]. We can isolate the  $D^*$  effects, however, by limiting the integration regions to the  $D^{*\pm}$  bands. Therefore, we calculate the effective rates

$$\Gamma_{B \rightarrow D^*(p_1 + p_2) \bar{D}(p_3)}^{\text{eff}} = \Gamma(B \rightarrow \pi^0(p_1) D(p_2) \bar{D}(p_3)) \Big|_{(M_{D^*} - \delta)^2 \leq s_{12} \leq (M_{D^*} + \delta)^2}, \quad (88)$$

in analogy to the effective  $B \rightarrow 3\pi$  rates in Eq. (63). Since the  $D^*$  width is very narrow, we can choose  $\delta = 5 \text{ MeV} \simeq 50 \Gamma_{D^{*+}}$ , which allows us to capture the  $D^*$  contributions and avoid those of  $D_{0,2}$ , which are about 400 MeV heavier than  $D^*$ . Thus we obtain

$$\begin{aligned} \mathcal{B}_{B^0 \rightarrow D^{*-} D^+}^{\text{eff}}[s_{+0} > s_{-0}] &= 0.98 \times 10^{-4}, & \mathcal{B}_{B^0 \rightarrow D^{*+} D^-}^{\text{eff}}[s_{+0} < s_{-0}] &= 1.14 \times 10^{-4}, \\ \mathcal{B}_{\bar{B}^0 \rightarrow D^{*-} D^+}^{\text{eff}}[s_{+0} > s_{-0}] &= 1.16 \times 10^{-4}, & \mathcal{B}_{\bar{B}^0 \rightarrow D^{*+} D^-}^{\text{eff}}[s_{+0} < s_{-0}] &= 0.98 \times 10^{-4}, \end{aligned} \quad (89)$$

where we note that our effective  $D\bar{D}\pi$  rates are about 3 times smaller than the corresponding two-body rates given in Table II, reflecting the empirical fact that  $\Gamma_{D^{*+} \rightarrow D\pi} \simeq 3 \Gamma_{D^{*+} \rightarrow D^+ \pi^0}$ .

The population asymmetry about the  $s_{+0} = s_{-0}$  line becomes

$$\mathcal{A}_{D\bar{D}\pi}^{+-} = \frac{\Gamma_{B, \bar{B} \rightarrow D^{*-} D^+}^{\text{eff}}[s_{+0} > s_{-0}] - \Gamma_{B, \bar{B} \rightarrow D^{*+} D^-}^{\text{eff}}[s_{+0} < s_{-0}]}{\Gamma_{B, \bar{B} \rightarrow D^{*-} D^+}^{\text{eff}}[s_{+0} > s_{-0}] + \Gamma_{B, \bar{B} \rightarrow D^{*+} D^-}^{\text{eff}}[s_{+0} < s_{-0}]} = +0.4\%, \quad (90)$$

which is the same as the result in Eq. (87). Since the  $D^*$  is so narrow, the population asymmetry can also be calculated directly from the the two-body rates in Table II, namely,

$$\mathcal{A}_{D\bar{D}\pi}^{+-} \simeq \frac{\Gamma_{B^0 \rightarrow D^{*-} D^+} + \Gamma_{\bar{B}^0 \rightarrow D^{*-} D^+} - \Gamma_{B^0 \rightarrow D^{*+} D^-} - \Gamma_{\bar{B}^0 \rightarrow D^{*+} D^-}}{\Gamma_{B^0 \rightarrow D^{*-} D^+} + \Gamma_{\bar{B}^0 \rightarrow D^{*-} D^+} + \Gamma_{B^0 \rightarrow D^{*+} D^-} + \Gamma_{\bar{B}^0 \rightarrow D^{*+} D^-}} = +0.4\%. \quad (91)$$

The  $D^{*\pm} D^\mp$  rates in this table are roughly consistent with data [58, 59]; in particular, we note the most precise measurement:  $\mathcal{B}(B \rightarrow D^{*\pm} D^\mp) = (8.8 \pm 1.0 \pm 1.3) \cdot 10^{-4}$  [59]. In this reference the time-integrated asymmetry is reported as well [59]:

$$\mathcal{A} = \frac{N_{D^{*+} D^-} - N_{D^{*-} D^+}}{N_{D^{*+} D^-} + N_{D^{*-} D^+}} = -0.03 \pm 0.11 \pm 0.05, \quad (92)$$

The Dalitz plot associated with the decay pathway  $B \rightarrow D^{*\pm} D^\mp \rightarrow D^+ D^- \pi^0$  gives rise to a CP-violating population asymmetry, though  $\Gamma_{D^{*+} \rightarrow D^0 \pi^+} \simeq 2 \Gamma_{D^{*+} \rightarrow D^+ \pi^0}$ . In this case, however, as we have seen, the  $D^*$  is so narrow that the population asymmetry is numerically indistinguishable from the untagged asymmetry computed from the two-body decay rates — there is no overlap region to treat. Consequently, the result of Eq. (92) can be compared with our estimate of the population asymmetry, to which it agrees, within errors.  $S_{D^* D}$  should yield  $\sin(2\beta)$  to a good approximation [50].

### C. $B_s \rightarrow D_s^+ D_s^- \pi^0$

We now consider the decays  $B_s^0, \bar{B}_s^0 \rightarrow D_s^{*\pm} D_s^\mp \rightarrow D_s^+ D_s^- \pi^0$ , in furtherment of the SM tests of Ref. [50]. As well known, the pertinent penguin contribution in  $B_s^0, \bar{B}_s^0 \rightarrow D_s^{*\pm} D_s^\mp$  decay possesses a subdominant weak phase, so that we expect its impact to be very small —  $S_{D_s^* D_s}$  should yield  $\sin(2\beta)$  to an excellent approximation. Were  $S_{D_s^* D_s}$  to differ significantly from  $\sin(2\beta)$ , the associated direct CP-violating observables would yield helpful insight into the nature of the emergent phenomena. The requisite formulas can be obtained from those in the  $B \rightarrow D^{*\pm} D^\mp \rightarrow D^\pm D^\mp \pi^0$  case by making the replacements

$$d \rightarrow s, \quad B \rightarrow B_s, \quad D^{(*)} \rightarrow D_s^{(*)}. \quad (93)$$

and by using the  $b \rightarrow s$  and  $\bar{b} \rightarrow \bar{s}$  entries in Table III, so that we do not report them explicitly. The CKM factors in the  $B_s^0 \rightarrow D_s^{*\pm} D_s^\mp$  amplitudes are  $V_{cb}^* V_{cs} \simeq A \lambda^2$  and  $V_{tb}^* V_{ts} \simeq -A \lambda^2$ , which are largely real, resulting in small CP violation. The  $D_s^*$  width has not been measured, but it is expected to be extremely small [60], of the order of 0.2 keV. As a consequence, the population asymmetry about the  $s_{+0} = s_{-0}$  line on the Dalitz plot for the  $D_s^+ D_s^- \pi^0$  final states can be calculated by using the  $B_s \rightarrow D_s^* D_s$  rates listed in Table II. Thus,

$$\mathcal{A}_{D_s \bar{D}_s \pi}^{+-} \simeq \frac{\Gamma_{B_s \rightarrow D^{*-} D^+} + \Gamma_{\bar{B}_s \rightarrow D^{*-} D^+} - \Gamma_{B_s \rightarrow D^{*+} D^-} - \Gamma_{\bar{B}_s \rightarrow D^{*+} D^-}}{\Gamma_{B_s \rightarrow D^{*-} D^+} + \Gamma_{\bar{B}_s \rightarrow D^{*-} D^+} + \Gamma_{B_s \rightarrow D^{*+} D^-} + \Gamma_{\bar{B}_s \rightarrow D^{*+} D^-}} = -0.03\%, \quad (94)$$

which is very small, in accord with SM expectations.

### D. $B_s \rightarrow K^+ K^- \pi^0$

As a final example, we consider  $B_s^0, \bar{B}_s^0 \rightarrow K^{*\pm} K^\mp \rightarrow K^+ K^- \pi^0$ ; the pertinent formulas are completely analogous to those in the  $B \rightarrow D^+ D^- \pi^0$  case. We need only make the replacements  $c \rightarrow u$  and  $d \rightarrow s$  for the quarks, and  $B \rightarrow B_s$  and  $D \rightarrow K$  for the mesons. The CP-odd combination  $a_g^* a_u + \bar{a}_g^* \bar{a}_u$  in this case is proportional to  $\sin \gamma$ , as can be inferred from the  $B_s \rightarrow K^{*\pm} K^\mp$  amplitudes in the Appendix.

Integrating over the two regions on the Dalitz plot for the  $K^+ K^- \pi^0$  final states, assuming no other contributions, we find

$$\mathcal{B}_{K \bar{K} \pi}^{(2)}[s_{+0} > s_{-0}] = 2.1 \times 10^{-7}, \quad \mathcal{B}_{K \bar{K} \pi} = 2 \mathcal{B}_{K \bar{K} \pi}^{(1)}[s_{+0} > s_{-0}] = 2.9 \times 10^{-6}, \quad (95)$$

which leads to

$$\mathcal{A}_{K\bar{K}\pi} = \frac{\Gamma_{K\bar{K}\pi}^{(2)}[s_{+0} > s_{-0}]}{\Gamma_{K\bar{K}\pi}^{(1)}[s_{+0} > s_{-0}]} = +15\% . \quad (96)$$

As we have discussed, it is better to consider effective branching ratios instead. Thus, taking  $\delta = 3\Gamma_{K^*}$ , we obtain

$$\begin{aligned} \mathcal{B}_{B_s^0 \rightarrow K^{*-} K^+}^{\text{eff}}[s_{+0} > s_{-0}] &= 0.09 \times 10^{-6} , & \mathcal{B}_{B_s^0 \rightarrow K^{*+} K^-}^{\text{eff}}[s_{+0} < s_{-0}] &= 1.00 \times 10^{-6} , \\ \mathcal{B}_{\bar{B}_s^0 \rightarrow K^{*-} K^+}^{\text{eff}}[s_{+0} > s_{-0}] &= 1.40 \times 10^{-6} , & \mathcal{B}_{\bar{B}_s^0 \rightarrow K^{*+} K^-}^{\text{eff}}[s_{+0} < s_{-0}] &= 0.10 \times 10^{-6} , \end{aligned} \quad (97)$$

where the effective  $K\bar{K}\pi$  rates are roughly 3 times smaller than the corresponding two-body rates in Table II, reflecting the isospin relation  $\Gamma_{K^{*+} \rightarrow K\pi} = 3\Gamma_{K^{*+} \rightarrow K^+\pi^0}$ . We thus find the population asymmetry

$$\mathcal{A}_{K\bar{K}\pi}^{+-} = \frac{\Gamma_{B_s, \bar{B}_s \rightarrow K^{*-} K^+}^{\text{eff}}[s_{+0} > s_{-0}] - \Gamma_{B_s, \bar{B}_s \rightarrow K^{*+} K^-}^{\text{eff}}[s_{+0} < s_{-0}]}{\Gamma_{B_s, \bar{B}_s \rightarrow K^{*-} K^+}^{\text{eff}}[s_{+0} > s_{-0}] + \Gamma_{B_s, \bar{B}_s \rightarrow K^{*+} K^-}^{\text{eff}}[s_{+0} < s_{-0}]} = +15\% . \quad (98)$$

This shows, once again, that focusing on the population asymmetry in the resonance regions on the Dalitz plot is sufficient to capture the CP-violating effect of interest. We note that our  $\mathcal{A}_{K\bar{K}\pi}^{+-}$  result is close to the value of  $\mathcal{A}_{CP}$  for  $B^0 \rightarrow K^{*+} K^-$  in Table II, and this is caused by the dominance of the  $B^0 \rightarrow K^{*+} K^-$  and  $\bar{B}^0 \rightarrow K^{*-} K^+$  contributions to the  $K^{*\pm}$  bands on the Dalitz plot.

## V. CONCLUSIONS

The study of direct CP violation in the  $B$ -meson system is needed to clarify the nature and origin of CP violation in nature. In this paper, we have studied a new tool: the population asymmetry in the untagged  $B_d, B_s$  decay rate to a self-conjugate final state of three pseudoscalar mesons. The population asymmetry emerges from the failure of mirror symmetry across the Dalitz plot; it signals the presence of direct CP violation. The amplitudes which give rise to such an asymmetry are of two, distinct classes. The first, proposed in Ref. [19], follows if we can separate the self-conjugate final state, via the resonances which appear, into distinct, CP-conjugate states; we term the latter CP-enantiomers. We note that such states are distinguishable by their location with respect to the mirror line of the Dalitz plot; in this sense they are distinguishable, mirror images. In this construction the angular momentum of the resonance with respect to the bachelor meson is fixed; such amplitudes form part of a more general class of amplitudes, for which the angular momentum of the two interfering amplitudes are of the same parity, as delineated in Eq. (42). The second class of amplitudes emerges from interfering amplitudes whose angular momentum is of differing parity, as delineated in Eq. (43). As an explicit example of the latter, we studied the CP-violation consequent to  $s$ -wave and  $p$ -wave interference, mediated by the  $\rho$  and  $\sigma$  resonances, in  $B \rightarrow \pi^+ \pi^- \pi^0$  decay. In our numerical examples, we find that the population asymmetry in the untagged decay rate is typically comparable in size to the partial rate asymmetries, making its measurement statistically advantageous.

The population asymmetry serves as a complementary assay to the study of the time-dependent asymmetry in neutral  $B$ -meson decays. In this regard, we have emphasized the SM tests discussed in Ref. [50], specifically the equality of the quantity  $S_f$ , induced by the interference of  $B - \bar{B}$  mixing and direct decay, for different modes mediated by  $b \rightarrow sc\bar{c}$ ,  $b \rightarrow ss\bar{s}$ , and  $b \rightarrow dc\bar{c}$  transitions. It is complementary in that it can simultaneously be regarded as a test that “polluting” SM amplitudes are indeed as small as expected, as well as a discriminant between different models of new physics, should the deviations from the SM predictions turn out to be large. One generally expects that physics beyond the standard model is most likely manifested through loop-level effects in  $B$  decays [50, 61]; new contributions may well enter neutral- $B$  mixing or the penguin part of the decay amplitudes, or both. Consequently, in the CP-violating observables we consider, new physics is most likely relegated to the penguin terms. In this regard, the determination of  $\mathcal{A}_{D_s\bar{D}_s\pi}^{+-}$  in  $B_s$  decay may be the most sensitive discriminant of emergent phenomena, as its asymmetry is expected, on general grounds, to be very small in the SM.

**Acknowledgments** S.G. and J.T. are supported by the U.S. Department of Energy under contracts DE-FG02-96ER40989 and DE-FG01-00ER45832. The work of J.T. was also supported by the Lightner-Sams Foundation. We thank J.A. Oller for the use of his scalar form factor program and T. Gershon and H. Quinn for helpful comments. S.G. thanks the Institute for Nuclear Theory at the University of Washington, Seattle and the SLAC Theory Group for hospitality during the completion of this work.

## APPENDIX

For the  $B \rightarrow \rho\pi$  amplitudes in Eq. (1), the relevant matrix elements in the framework of Ref. [34] are

$$\begin{aligned} \langle \pi^+(p) | \bar{u} \gamma_\mu L d | 0 \rangle &= \langle \pi^-(p) | \bar{d} \gamma_\mu L u | 0 \rangle = i f_\pi p_\mu , \\ \langle \rho^+(p, \varepsilon) | \bar{u} \gamma_\mu d | 0 \rangle &= \langle \rho^-(p, \varepsilon) | \bar{d} \gamma_\mu u | 0 \rangle = f_\rho M_\rho \varepsilon_\mu^* , \end{aligned} \quad (99)$$

$$\begin{aligned} q^\mu \langle \rho^+(p, \varepsilon) | \bar{u} \gamma_\mu L b | \bar{B}^0(k) \rangle &= -2i A_0^{B \rightarrow \rho}(q^2) M_\rho \varepsilon^* \cdot q , \\ \langle \pi^+(p) | \bar{u} \gamma^\mu L b | \bar{B}^0(k) \rangle &= (k + p)^\mu F_1^{B \rightarrow \pi}(q^2) + \frac{M_B^2 - M_\pi^2}{q^2} q^\mu (F_0^{B \rightarrow \pi}(q^2) - F_1^{B \rightarrow \pi}(q^2)) , \end{aligned} \quad (100)$$

where  $L \equiv 1 - \gamma_5$ ,  $q \equiv k - p$ ,  $f_\pi$  and  $f_\rho$  are the usual decay constants, and  $A_0(q^2)$  and  $F_{0,1}(q^2)$  are form factors. In our phase convention for the meson flavor wave-functions,  $\bar{B}^0 = b\bar{d}$ ,  $\pi^+ = u\bar{d}$ ,  $\sqrt{2}\pi^0 = u\bar{u} - d\bar{d}$ ,  $\pi^- = d\bar{u}$ , with the same convention for the  $\rho$ . Then, using isospin symmetry, we also have  $\langle \pi^+ | \bar{u} \gamma^\mu L d | 0 \rangle = \sqrt{2} \langle \pi^0 | \bar{u} \gamma^\mu L u | 0 \rangle$  and  $\langle \pi^+ | \bar{u} \gamma^\mu b | \bar{B}^0 \rangle = -\sqrt{2} \langle \pi^0 | \bar{d} \gamma^\mu b | \bar{B}^0 \rangle$ . The resulting

amplitudes for  $\bar{B}^0 \rightarrow \rho\pi$  are

$$\begin{aligned}
\bar{a}_{+-} &= \sqrt{2} G_F \left\{ \lambda_u^{(d)} a_1 - \lambda_t^{(d)} \left[ a_4 + a_{10} - (a_6 + a_8) R_{\pi^-} \right] \right\} f_\pi M_\rho A_0^{B \rightarrow \rho}(M_\pi^2) , \\
\bar{a}_{-+} &= \sqrt{2} G_F \left[ \lambda_u^{(d)} a_1 - \lambda_t^{(d)} (a_4 + a_{10}) \right] f_\rho M_\rho F_1^{B \rightarrow \pi}(M_\rho^2) , \\
\bar{a}_{00} &= \frac{-G_F}{\sqrt{2}} \left\{ \lambda_u^{(d)} a_2 + \lambda_t^{(d)} \left[ a_4 + \frac{3}{2}a_7 - \frac{3}{2}a_9 - \frac{1}{2}a_{10} - (a_6 - \frac{1}{2}a_8) R_{\pi^0} \right] \right\} f_\pi M_\rho A_0^{B \rightarrow \rho}(M_\pi^2) \\
&\quad - \frac{G_F}{\sqrt{2}} \left[ \lambda_u^{(d)} a_2 + \lambda_t^{(d)} \left( a_4 - \frac{3}{2}a_7 - \frac{3}{2}a_9 - \frac{1}{2}a_{10} \right) \right] f_\rho M_\rho F_1^{B \rightarrow \pi}(M_\rho^2) ,
\end{aligned} \tag{101}$$

where the numerical values of  $a_i$  for  $b \rightarrow d$  decay are obtained from Table III,  $R_{\pi^-} \equiv 2M_{\pi^-}^2 / [(m_u + m_b)(m_u + m_d)]$ , and  $R_{\pi^0} \equiv M_{\pi^0}^2 / [(m_d + m_b)m_d]$ . The amplitudes  $a_{kl}$  for  $B^0 \rightarrow \rho\pi$  can be found from  $\bar{a}_{lk}$  by replacing  $\lambda_{q'}^{(q)}$  with  $\lambda_{q'}^{(q)*}$  and using the  $\bar{b} \rightarrow \bar{d}$  entries in Table III.

Turning to the  $B \rightarrow \rho\pi \rightarrow 3\pi$  amplitudes in Eqs. (2,4),<sup>9</sup> we note that they contain the  $\rho \rightarrow \pi\pi$  vertex function  $\Gamma_{\rho\pi\pi}(s)$ , which is given by

$$\Gamma_{\rho\pi\pi}(s) = \frac{-F_\rho(s)}{f_{\rho\gamma}} , \tag{102}$$

where  $F_\rho(s)$  is the vector form-factor of the pion and  $f_{\rho\gamma}$  is the  $\rho\gamma$  coupling constant. The form factor  $F_\rho(s)$  is determined by fitting to  $e^+e^- \rightarrow \pi^+\pi^-$  data with a parametrization consistent with theoretical constraints [62]. The value of  $f_{\rho\gamma}$  is determined from the  $\rho \rightarrow e^+e^-$  width, which, in turn, is extracted from the  $e^+e^- \rightarrow \pi^+\pi^-$  cross section at  $s = M_\rho^2$  [63]. The overall sign is chosen so that Eq. (102) to be that of the Breit-Wigner (BW) form,

$$\Gamma_{\rho\pi\pi}^{\text{BW}}(s) = \frac{g_{\rho\pi\pi}}{s - M_\rho^2 + i\Gamma_\rho M_\rho} \tag{103}$$

as  $s \rightarrow M_\rho^2$ , where  $g_{\rho\pi\pi}$  is the  $\rho \rightarrow \pi\pi$  coupling constant. In our numerical analysis, we employ the “solution  $B$ ” fit of Ref. [62] for  $F_\rho(s)$ , for which  $f_{\rho\gamma} = 0.122 \pm 0.001 \text{ GeV}^2$  [63]. For  $s \geq (M_\pi + M_\omega)^2$  we match  $\Gamma_{\rho\pi\pi}(s)$  to the BW expression, as the fit for  $F_\rho(s)$  exists exclusively in the region where  $\pi\pi$  scattering is elastic, see Refs. [48, 49] for further details.

To incorporate the  $B \rightarrow \sigma\pi^0$  contributions, we need the additional matrix element

$$q^\mu \langle \sigma(p) | \bar{d}\gamma_\mu Lb | \bar{B}^0(k) \rangle = -i(M_B^2 - M_\sigma^2) F_0^{B \rightarrow \sigma}(q^2) . \tag{104}$$

It follows that the  $\bar{B}^0 \rightarrow \sigma\pi^0$  amplitude in Eq. (67) is

$$\begin{aligned}
\bar{a}_\sigma &= \frac{G_F}{2} \left\{ \lambda_u^{(d)} a_2 + \lambda_t^{(d)} \left[ a_4 + \frac{3}{2}a_7 - \frac{3}{2}a_9 - \frac{1}{2}a_{10} - (a_6 - \frac{1}{2}a_8) R_{\pi^0} \right] \right\} (M_{B^0}^2 - M_\sigma^2) f_\pi F_0^{B \rightarrow \sigma}(M_\pi^2) \\
&\quad - G_F \lambda_t^{(d)} (a_6 - \frac{1}{2}a_8) \frac{\langle \sigma | \bar{d}d | 0 \rangle}{m_b - m_d} (M_{B^0}^2 - M_{\pi^0}^2) F_0^{B \rightarrow \pi}(M_\sigma^2) ,
\end{aligned} \tag{105}$$

<sup>9</sup> The signs of the different terms in Eq. (4) follow from the  $\rho \rightarrow \pi\pi$  couplings  $\langle \pi^0(p_0) \pi^\pm(p_\pm) | \rho^\pm \rangle = \pm g_{\rho\pi\pi} \varepsilon_\rho \cdot (p_0 - p_\pm)$  and  $\langle \pi^+(p_+) \pi^-(p_-) | \rho^0 \rangle = g_{\rho\pi\pi} \varepsilon_\rho \cdot (p_+ - p_-)$ , where we adopt the notation  $\langle M_2 M_3 | M_1 \rangle \equiv \langle M_2 M_3 | \mathcal{H}_{\text{strong}} | M_1 \rangle$ . The signs of these couplings follow, in turn, from the phase convention we have chosen for the flavor wave-functions:  $|\pi^\pm\rangle = \mp |I=1, I_3=\pm 1\rangle$  and  $|\pi^0\rangle = |I=1, I_3=0\rangle$ , etc.

TABLE III: Numerical values of the coefficients  $a_i$  with  $N_c = 3$ , reproduced from Tables VI and VII in Ref. [34], for  $b \rightarrow q$  and  $\bar{b} \rightarrow \bar{q}$  transitions, with  $q = d, s$ . Each of the entries for  $a_3, \dots, a_{10}$  ought to be multiplied by a factor of  $10^{-4}$ .

	$b \rightarrow d$	$\bar{b} \rightarrow \bar{d}$	$b \rightarrow s$	$\bar{b} \rightarrow \bar{s}$
$a_1$	1.05	1.05	1.05	1.05
$a_2$	0.053	0.053	0.053	0.053
$a_3$	48	48	48	48
$a_4$	$-412 - 36i$	$-461 - 124i$	$-439 - 77i$	$-431 - 77i$
$a_5$	-45	-45	-45	-45
$a_6$	$-548 - 36i$	$-597 - 124i$	$-575 - 77i$	$-568 - 77i$
$a_7$	$0.7 - 1.0i$	$0.3 - 1.8i$	$0.5 - 1.3i$	$0.5 - 1.3i$
$a_8$	$4.7 - 0.3i$	$4.5 - 0.6i$	$4.6 - 0.4i$	$4.6 - 0.4i$
$a_9$	$-94 - 1.0i$	$-95 - 1.8i$	$-94 - 1.3i$	$-94 - 1.3i$
$a_{10}$	$-14 - 0.3i$	$-14 - 0.6i$	$-14 - 0.4i$	$-14 - 0.4i$

where we use  $M_\sigma = 478$  MeV determined in Ref. [64],  $F_0^{B \rightarrow \sigma}(M_\pi^2) = 0.46$  as per Refs. [47], and  $\langle \sigma | \bar{d}d | 0 \rangle = 2M_{\pi^+}^2 / [\sqrt{6} \chi (m_u + m_d)]$ , with  $\chi = 20.0 \text{ GeV}^{-1}$  [49]. To obtain the  $\bar{B}^0 \rightarrow \sigma \pi^0$  amplitude, we note that  $CP|\rho^0 \pi^0\rangle = +|\rho^0 \pi^0\rangle$  and  $CP|\sigma \pi^0\rangle = -|\sigma \pi^0\rangle$  for  $B \rightarrow \rho \pi, \sigma \pi$ , as the relative angular-momenta in the final states are  $l = 1$  and  $0$ , respectively. Consequently,  $a_\sigma$  can be found from  $\bar{a}_\sigma$  by replacing  $\lambda_{q'}^{(q)}$  with  $\lambda_{q'}^{(q)*}$ , using the  $\bar{b} \rightarrow \bar{d}$  entries in Table III, and adding an overall minus sign, which is consistent with Eq. (71).

The  $\sigma$  contribution to the  $B \rightarrow 3\pi$  amplitudes in Eq. (68) involve the function  $f_\sigma(s) = \Gamma_{\sigma\pi\pi}(s)$ , which describes the  $\sigma \rightarrow \pi\pi$  vertex function in the isospin  $I = 0$  and angular-momentum  $J = 0$  channel. This function must satisfy known theoretical constraints [49], and we adopt

$$\Gamma_{\sigma\pi\pi}(s) = \chi \Gamma_1^{n*}(s) , \quad (106)$$

for our numerical work, where the function  $\Gamma_1^n(s)$  is computed in Ref. [65]. We remark that the theoretically consistent  $\Gamma_{\sigma\pi\pi}(s)$  is very different from the Breit-Wigner form used in Ref. [64], as detailed in Ref. [49].

For the  $B \rightarrow D^{*\pm} D^\mp$  amplitudes in Eq. (80), the needed matrix elements are analogous to those of the  $\rho\pi$  case, where the replacement of the  $u$  with  $c$  quarks is realized throughout. Thus for  $\bar{B}^0 \rightarrow D^* D$  decay, we have

$$\begin{aligned} \bar{a}_{+-} &= \sqrt{2} G_F \left\{ \lambda_c^{(d)} a_1 - \lambda_t^{(d)} \left[ a_4 + a_{10} - (a_6 + a_8) R_D \right] \right\} f_D M_{D^*} A_0^{B \rightarrow D^*}(M_D^2) , \\ \bar{a}_{-+} &= \sqrt{2} G_F \left[ \lambda_c^{(d)} a_1 - \lambda_t^{(d)} (a_4 + a_{10}) \right] f_{D^*} M_{D^*} F_1^{B \rightarrow D}(M_{D^*}^2) , \end{aligned} \quad (107)$$

where  $R_D \equiv 2M_D^2 / [(m_c + m_b)(m_c + m_d)]$ . For the form factors, we use [66]

$$2 F_1^{B \rightarrow D}(q^2) = \frac{m_B + m_D}{\sqrt{m_B m_D}} \xi(w) , \quad 2 A_0^{B \rightarrow D^*}(q^2) = \frac{m_B + m_{D^*}}{\sqrt{m_B m_{D^*}}} \xi(w) , \quad (108)$$

where

$$\xi(w) = \left( \frac{2}{1+w} \right)^2, \quad w = \frac{m_B^2 + m_{D^{(*)}}^2 - q^2}{2 m_B m_{D^{(*)}}}. \quad (109)$$

The amplitudes  $a_{kl}$  for  $B^0 \rightarrow D^* D$  decay are obtained from  $\bar{a}_{lk}$  by replacing  $\lambda_{q'}^{(q)}$  with  $\lambda_{q'}^{(q)*}$  and using the  $\bar{b} \rightarrow \bar{d}$  entries in Table III.

The  $B \rightarrow D^\pm D^\mp \pi^0$  amplitudes in Eq. (81) contain the functions

$$f_\pm = \frac{\pm \frac{1}{2} g_{D^* D \pi}}{s_{\pm 0} - m_{D^*}^2 + i\Gamma_{D^*} m_{D^*}} \left[ s_{+-} - s_{\mp 0} - m_D^2 + m_\pi^2 - (m_{B_s}^2 - s_{\pm 0} - m_D^2) \frac{m_D^2 - m_\pi^2}{m_{D^*}^2} \right], \quad (110)$$

where  $g_{D^* D \pi}$  is the coupling constant associated with the strong decays  $D^{*\pm} \rightarrow D^\pm \pi^0$ ,

$$\mathcal{M}_{D^{*\pm} \rightarrow D^\pm \pi^0} = \pm 2 g_{D^* D \pi} \varepsilon \cdot p_\pi. \quad (111)$$

From the empirical values  $\mathcal{B}(D^{*+} \rightarrow D^+ \pi^0) = (30.7 \pm 0.5)\%$  [67] and  $\Gamma_{D^{*+}} = (96 \pm 4 \pm 22)\text{keV}$ , [68] we extract  $g_{D^* D \pi} = 6.3$ . The use of the Breit-Wigner form for the  $D^*$  resonance in Eq. (110) is appropriate as the  $D^*$  is narrow.

The  $B \rightarrow K^{*\pm} K^\mp$  amplitudes also follow from the  $\rho\pi$  case, and thus we have for  $\bar{B}^0 \rightarrow K^{*\pm} K^\mp$

$$\begin{aligned} \bar{a}_{+-} &= \sqrt{2} G_F \left\{ \lambda_u^{(s)} a_1 - \lambda_t^{(s)} \left[ a_4 + a_{10} - (a_6 + a_8) R_K \right] \right\} f_K M_{K^*} A_0^{B \rightarrow K^*}(M_K^2), \\ \bar{a}_{-+} &= \sqrt{2} G_F \left[ \lambda_u^{(s)} a_1 - \lambda_t^{(s)} (a_4 + a_{10}) \right] f_{K^*} M_{K^*} F_1^{B \rightarrow K}(M_{K^*}^2), \end{aligned} \quad (112)$$

where the  $a_i$  values for  $b \rightarrow s$  decay are given in Table III and  $R_K \equiv 2M_K^2/[(m_u + m_b)(m_u + m_s)]$ . The amplitudes  $a_{kl}$  for  $B^0 \rightarrow K^{*\pm} K^\mp$  follow from  $\bar{a}_{lk}$  by replacing  $\lambda_{q'}^{(q)}$  with  $\lambda_{q'}^{(q)*}$  and using the  $\bar{b} \rightarrow \bar{s}$  entries in Table III. The  $K^{*\pm} \rightarrow K^\pm \pi^0$  coupling constant occurring in the analogue of  $f_\pm$  in Eq. (110) is  $g_{K^* K \pi} = 3.2$ , and extracted using the measured  $K^{*+}$  width [67] and the isospin relation  $\Gamma_{K^{*+} \rightarrow K \pi} = 3 \Gamma_{K^{*+} \rightarrow K^+ \pi^0}$ .

Finally, we list all the input parameters which have not been previously mentioned. For the heavy mesons, we have

$$\begin{aligned} M_{B^0} &= 5.2794 \text{ GeV}, & \tau_{B^0} &= 1.548 \times 10^{-12} \text{ s}, \\ M_{B_s^0} &= 5.3696 \text{ GeV}, & \tau_{B_s^0} &= 1.493 \times 10^{-12} \text{ s}, \\ f_D &= 200 \text{ MeV}, & M_{D^\pm} &= 1869.3 \text{ MeV}, & f_{D^*} &= 230 \text{ MeV}, & M_{D^{*\pm}} &= 2010.0 \text{ MeV}, \\ f_{D_s} &= 240 \text{ MeV}, & M_{D_s^\pm} &= 1968.6 \text{ MeV}, & f_{D_s^*} &= 275 \text{ MeV}, & M_{D_s^{*\pm}} &= 2112.4 \text{ MeV}, \end{aligned} \quad (113)$$

and for the light mesons

$$\begin{aligned} f_\pi &= 134 \text{ MeV}, & M_{\pi^\pm} &= 139.57 \text{ MeV}, & M_{\pi^0} &= 134.98 \text{ MeV}, \\ f_\rho &= 210 \text{ MeV}, & M_\rho &= 769.3 \text{ MeV}, & \Gamma_\rho &= 150 \text{ MeV}, & g_{\rho\pi\pi} &= 5.8, \\ f_K &= 158 \text{ MeV}, & M_{K^\pm} &= 493.68 \text{ MeV}, \\ f_{K^*} &= 214 \text{ MeV}, & M_{K^{*\pm}} &= 891.66 \text{ MeV}, & \Gamma_{K^{*\pm}} &= 50.8 \text{ MeV}, \end{aligned} \quad (114)$$

where the decay constants have been obtained from Ref. [69]. For current quark masses, we use the running values at  $\mu = 2.5$  GeV found in Ref. [34]:

$$\begin{aligned} m_u &= 4.2 \text{ MeV} , & m_d &= 7.6 \text{ MeV} , & m_s &= 122 \text{ MeV} , \\ m_c &= 1.5 \text{ GeV} , & m_b &= 4.88 \text{ GeV} , \end{aligned} \quad (115)$$

For the heavy-to-light form factors, we employ

$$\begin{aligned} A_0^{B \rightarrow \rho}(M_\pi^2) &\simeq A_0^{B \rightarrow \rho}(0) = 0.28 , & F_1^{B \rightarrow \pi}(M_\rho^2) &\simeq F_1^{B \rightarrow \pi}(0) = 0.33 , \\ F_0^{B \rightarrow \pi}(M_\sigma^2) &\simeq F_0^{B \rightarrow \pi}(0) = 0.33 , \\ A_0^{B_s \rightarrow K^*}(M_K^2) &\simeq A_0^{B_s \rightarrow K^*}(0) = 0.24 , & F_1^{B_s \rightarrow K}(M_{K^*}^2) &\simeq F_1^{B_s \rightarrow K}(0) = 0.27 , \end{aligned} \quad (116)$$

estimated in the BSW model [70].

---

[1] B. Aubert *et al.* [BABAR Collaboration], Phys. Rev. Lett. **87**, 091801 (2001); K. Abe *et al.* [Belle Collaboration], *ibid.* **87**, 091802 (2001).

[2] N. Cabibbo, Phys. Rev. Lett. **10** (1963) 531; M. Kobayashi and T. Maskawa, Prog. Theor. Phys. **49** (1973) 652.

[3] A. Höcker, H. Lacker, S. Laplace, and F. Le Diberder, Eur. Phys. J. C **21**, 225 (2001); for an update, note S. Laplace, arXiv:hep-ph/0209188, as well as <http://www.ckmfitter.in2p3.fr>.

[4] L. Wolfenstein, Phys. Rev. Lett. **51**, 1945 (1983).

[5] The sign of  $\sin \delta_{\text{KM}}$  predicates whether  $\alpha$ ,  $\beta$ , and  $\gamma$  are the internal or external angles of the unitarity triangle in the SM, as detailed in Y. Nir and H.R. Quinn, Phys. Rev. D **42**, 1473 (1990). If  $\sin \delta_{\text{KM}} > 0$ , as currently believed, the angles are internal.

[6] L. Wolfenstein, Phys. Rev. Lett. **13**, 562 (1964).

[7] L. Wolfenstein, in J.L. Rosner and B.D. Winstein, *Kaon Physics* (University of Chicago Press, Chicago, 2001).

[8] L. Wolfenstein, arXiv:hep-ph/0210025.

[9] I.I. Bigi, Phys. Lett. B **535**, 155 (2002).

[10] S. Chen *et al.* [CLEO Collaboration], Phys. Rev. Lett. **85**, 525 (2000); B. Aubert *et al.* [BABAR Collaboration], *ibid.* **65**, 051101 (2002); B. Aubert *et al.* [BABAR Collaboration], arXiv:hep-ex/0206053.

[11] B. C. Casey *et al.* [Belle Collaboration], Phys. Rev. D **66**, 092002 (2002); Y. Unno *et al.* [Belle Collaboration], Phys. Rev. D **68**, 011103 (2003).

[12] B. Aubert *et al.* [BABAR Collaboration], Phys. Rev. Lett. **89**, 281802 (2002); B. Aubert *et al.* [BABAR Collaboration], *ibid.* **89**, 281802 (2002).

[13] L. Wolfenstein, Nucl. Phys. B **246**, 45 (1984); B. Winstein and L. Wolfenstein, Rev. Mod. Phys. **65**, 1113 (1993).

[14] K. Abe *et al.* [Belle Collaboration], Phys. Rev. Lett. **89**, 071801 (2002); B. Aubert *et al.* [BABAR Collaboration], Phys. Rev. Lett. **89**, 281802 (2002).

[15] B. Aubert *et al.* [BABAR Collaboration], arXiv:hep-ex/0207070; K. Abe *et al.* [Belle Collaboration], arXiv:hep-ex/0207098.

- [16] B. Winstein, Phys. Rev. Lett. **68**, 1271 (1992).
- [17] L. Wolfenstein and F. Wu, Europhys. Lett. **58**, 49 (2002).
- [18] N. Sinha and R. Sinha, Phys. Rev. Lett. **80**, 3706 (1998).
- [19] S. Gardner, Phys. Lett. B **553**, 261 (2003).
- [20] A. B. Carter and A. I. Sanda, Phys. Rev. Lett. 45 (1980) 952; Phys. Rev. D 23 (1981) 1567.
- [21] I. I. Bigi and A. I. Sanda, Nucl. Phys. B 193 (1981) 85; Nucl. Phys. B 281 (1987) 41.
- [22] I. Dunietz and J. L. Rosner, Phys. Rev. D 34 (1986) 1404.
- [23] P.F. Harrison and H.R. Quinn [BABAR Collaboration], *The BaBar Physics Book*, SLAC-R-0504, <http://www.slac.stanford.edu/pubs/slacreports/slac-r-504.html>.
- [24] John D. Roberts and Marjorie C. Caserio, *Basic Principles in Organic Chemistry*, 2nd ed., W. A. Benjamin, Inc., Menlo Park, CA, 1977.
- [25] A.E. Snyder and H.R. Quinn, Phys. Rev. D **48**, 2139 (1993).
- [26] H.R. Quinn and J.P. Silva, Phys. Rev. D **62**, 054002 (2000).
- [27] I.I. Bigi, V.A. Khoze, N.G. Uraltsev, and A.I. Sanda, in *CP Violation*, ed. C. Jarlskog (World Scientific, Singapore, 1989) and references therein.
- [28] K. Anikeev *et al.*, arXiv:hep-ph/0201071.
- [29] I.I. Bigi and A.I. Sanda, Nucl. Phys. B **281**, 41 (1987).
- [30] R. Aleksan, A. Le Yaouanc, L. Oliver, O. Pène, and J. C. Raynal, Phys. Lett. B **316**, 567 (1993).
- [31] M. Beneke, G. Buchalla, and I. Dunietz, Phys. Rev. D **54**, 4419 (1996).
- [32] C. Zemach, Phys. Rev. **133**, B1201 (1964).
- [33] G. Valencia, Phys. Rev. D **39**, 3339 (1989).
- [34] A. Ali, G. Kramer, and C.D. Lu, Phys. Rev. D **58**, 094009 (1998); Phys. Rev. D **59**, 014005 (1999).
- [35] H.Y. Cheng and K.C. Yang, Phys. Rev. D **62**, 054029 (2000).
- [36] M.Z. Yang and Y.D. Yang, Phys. Rev. D **62**, 114019 (2000).
- [37] D.s. Du, H.j. Gong, J.f. Sun, D.s. Yang and G.h. Zhu, Phys. Rev. D **65**, 094025 (2002) [Erratum-*ibid.* D **66**, 079904 (2002)].
- [38] M. Beneke and M. Neubert, arXiv:hep-ph/0308039.
- [39] A. Höcker, M. Laget, S. Laplace, and J. v. Wimmersperg-Toeller, *Using Flavor Symmetry to Constrain  $\alpha$  from  $B \rightarrow \rho\pi$* , LAL 03-17, BaBar Analysis Document #628, <http://www.slac.stanford.edu/~laplace/doc/lal-03-17.ps.gz>
- [40] G. Buchalla, A.J. Buras, and M.E. Lautenbacher, Rev. Mod. Phys. **68**, 1125 (1996).
- [41] A. Ali and C. Greub, Phys. Rev. D **57**, 2996 (1998); H.-Y. Cheng and B. Tseng, *ibid.* **58**, 094005 (1998); Y.-H. Chen, H.-Y. Cheng, B. Tseng, and K.-C. Yang, *ibid.* **60**, 094014 (1999); H.-Y. Cheng and K.-C. Yang, *ibid.* **62**, 054029 (2000).
- [42] C.P. Jessop *et al.* [CLEO Collaboration], Phys. Rev. Lett. **85**, 2881 (2000).
- [43] B. Aubert *et al.* [BABAR Collaboration], arXiv:hep-ex/0306030.
- [44] A. Gordon *et al.* [Belle Collaboration], Phys. Lett. B **542**, 183 (2002); K. Abe *et al.* [Belle Collaboration], arXiv:hep-ex/0307077.
- [45] H. Jawahery, talk at Lepton-Photon 2003, August 11-16, 2003, Fermilab, Batavia, IL, [http://conferences.fnal.gov/lp2003/program/S5/jawahery\\_S05.pdf](http://conferences.fnal.gov/lp2003/program/S5/jawahery_S05.pdf)
- [46] A. Deandrea *et al.*, Phys. Rev. D **62**, 036001 (2000).
- [47] A. Deandrea and A.D. Polosa, Phys. Rev. Lett. **86**, 216 (2001).
- [48] J. Tandean and S. Gardner, Phys. Rev. D **66**, 034019 (2002).
- [49] S. Gardner and U.-G. Meißner, Phys. Rev. D **65**, 094004 (2002).
- [50] Y. Grossman and M. P. Worah, Phys. Lett. B **395**, 241 (1997).

- [51] M. Gronau, Phys. Lett. B **233**, 479 (1989).
- [52] R. Aleksan, I. Dunietz, B. Kayser, and F. Le Diberder, Nucl. Phys. B **361**, 141 (1991).
- [53] R. Aleksan, A. Le Yaouanc, L. Oliver, O. Pène, and J.C. Raynal, Phys. Lett. B **317**, 173 (1993).
- [54] A. Garmash *et al.* [Belle Collaboration], arXiv:hep-ex/0307082; arXiv:hep-ex/0308035.
- [55] M. Gronau and J. L. Rosner, Phys. Lett. B **564**, 90 (2003).
- [56] Y. Grossman, Z. Ligeti, Y. Nir, and H. Quinn, Phys. Rev. D **68**, 015004 (2003).
- [57] J. Charles *et al.*, Phys. Lett. B **425**, 375 (1998); *ibid.* **433**, 441(E) (1998); P. Colangelo *et al.*, Phys. Rev. D **60**, 033002 (1999).
- [58] E. Lipeles *et al.* [CLEO Collaboration], Phys. Rev. D **62**, 032005 (2000); K. Abe *et al.* [Belle Collaboration], Phys. Rev. Lett. **89**, 122001 (2002).
- [59] B. Aubert *et al.* [BABAR Collaboration], Phys. Rev. Lett. **90**, 221801 (2003).
- [60] J.L. Goity and W. Roberts, Phys. Rev. D **64**, 094007 (2001).
- [61] For reviews, note Y. Nir and H. R. Quinn, Ann. Rev. Nucl. Part. Sci. **42**, 211 (1992); I. Dunietz, Annals Phys. **184**, 350 (1988), as well as, e.g., J. Liu and L. Wolfenstein, Phys. Lett. B **197**, 536 (1987); Y. Nir and D. J. Silverman, Nucl. Phys. B **345**, 301 (1990); C. Dib, D. London, and Y. Nir, Int. J. Mod. Phys. A **6**, 1253 (1991); T. Goto, N. Kitazawa, Y. Okada, and M. Tanaka, Phys. Rev. D **53**, 6662 (1996); N. G. Deshpande, B. Dutta, and S. Oh, Phys. Rev. Lett. **77**, 4499 (1996); J. P. Silva and L. Wolfenstein, Phys. Rev. D **55**, 5331 (1997); M. P. Worah, Phys. Rev. D **54**, 2198 (1996); M. Gronau and D. London, Phys. Rev. D **55**, 2845 (1997).
- [62] S. Gardner and H.B. O'Connell, Phys. Rev. D **59**, 076002 (1999).
- [63] S. Gardner and H.B. O'Connell, Phys. Rev. D **57**, 2716 (1998); *ibid.* **62**, 019903(E) (1999).
- [64] E.M. Aitala *et al.* [E791 Collaboration], Phys. Rev. Lett. **86**, 770 (2001).
- [65] U.-G. Meißner and J.A. Oller, Nucl. Phys. A **679**, 671 (2001).
- [66] M. Neubert, Phys. Rept. **245**, 259 (1994); V. Morenas *et al.*, Phys. Rev. D **56**, 5668 (1997).
- [67] D.E. Groom *et al.* [Particle Data Group Collaboration], Eur. Phys. J. C **15**, 1 (2000).
- [68] S. Ahmed *et al.* [CLEO Collaboration], Phys. Rev. Lett. **87**, 251801 (2001); A. Anastassov *et al.* [CLEO Collaboration], Phys. Rev. D **65**, 032003 (2002).
- [69] M. Neubert and B. Stech, in A.J. Buras and M. Lindner, *Heavy Flavours II* (World Scientific, Singapore, 1998).
- [70] M. Bauer, B. Stech, and M. Wirbel, Z. Phys. C **34**, 103 (1987). The  $B_s \rightarrow K^{(*)}$  form factors are calculated in the BSW model by D. Du and Z.-Z. Xing, Phys. Rev. D **48**, 3400 (1993).